In presenting the dissertation as a partial fulfillment of the requirements for an advanced degree from the Georgia Institute of Technology, I agree that the Library of the Institute shall make it available for inspection and circulation in accordance with its regulations governing materials of this type. I agree that permission to copy from, or to publish from, this dissertation may be granted by the professor under whose direction it was written, or, in his absence, by the Dean of the Graduate Division when such copying or publication is solely for scholarly purposes and does not involve potential financial gain. It is understood that any copying from, or publication of, this dissertation which involves potential financial gain will not be allowed without written permission.

7/25/68

DETERMINATION OF THE EFFECTS OF ELECTROMAGNETIC ENERGIES ON THE HEMATOLOGIC SYSTEM

A THESIS

Presented to

The Faculty of the Division of Graduate Studies and Research

by

Richard Frederick Boggs

In Partial Fulfillment

of the Requirements for the Degree

Doctor of Philosophy

in the School of Nuclear Engineering

Georgia Institute of Technology

February, 1971

DETERMINATION OF THE EFFECTS OF ELECTROMAGNETIC ENERGIES ON THE HEMATOLOGIC SYSTEM

Approved:

Chairman

Date Approved by Chairman: _____

TABLE OF CONTENTS

ACKNOWLEDGMENTS

I wish to express my sincere appreciation to Mr. John C. Villforth, Director of the U.S. Public Health Service, Bureau of Radiological Health, who has been a constant inspiration to me for eleven years, and without whose guidance, encouragement, and approvals, my graduate education would not have been possible.

I am also most appreciative for the invaluable encouragement and assistance, both technical and administrative, that I received throughout the research and preparation of the thesis from my thesis advisor, Dr. Albert P. Sheppard, Head, Special Techniques Branch, Electronics Division.

I also wish to thank Dr. Nancy W. Walls, Associate Professor of Biology, and Dr. Don S. Harmer, Professor of Physics and Nuclear Engineering, for their assistance and suggestions while serving as members of my reading committee.

I am especially grateful to Miss Jeanne Clark for providing the preparation and laboratory analysis of the blood samples.

I am deeply indebted to the following individuals who relieved me periodically by donating blood used for this research: Miss Jeanne Clark; my wife, Mrs. Ardith Boggs; Mr. Gary Altman; Mr. Joseph Allen, Miss Wanda Baugus; Miss Frances Clemmer; Dr. Floyd James; and Miss Carolyn Kitchens.

I am grateful to the following persons from Georgia Tech who provided assistance and support for this investigation: Dr. Walter Bloom and Messrs. Harold Bassett, Robert Shackelford, Keith Huddleston,

William Fife, and George Ewell.

Thanks is given to the following individuals from the PHS, Bureau of Radiological Health, for obtaining supplemental support and other assistance: Dr. Robert Elder, and Messrs. Robert Sauer, William Link, and Walter Gundaker.

I am grateful to Dr. Carlyle Roberts, Director, School of Nuclear Engineering, for his cooperation and understanding, to Dr. Spencer Brewer, Piedmont Hospital, Atlanta, for his consultations, and to Mrs. Mary Bryant and Mrs. Susan Harden for their efficient typing and editing.

Finally, and most importantly, I am extremely grateful to my wife for putting up with all the headaches and frustrations, and for providing the constant encouragement needed in order to complete my graduate studies.

LIST OF TABLES

LIST OF ILLUSTRATIONS

Page

SUMMARY

At the present time there is much uncertainty as to what constitutes a safe personnel exposure level for microwave radiation. The most frequently used level of 10 mW/cm^2 for continuous exposure in the United States is a factor of 10^3 higher than the level established in the U.S.S.R. One of the major reasons for such a large discrepancy appears to result from (1) an inability to evaluate studies performed in the U.S.S.R., (2) a lack of knowledge on biological effects from low-level exposures to biological systems, and (3) inaccuracies in the measurement techniques used in research on effects from microwaves.

It was the purpose of this research to design and fabricate a relatively inexpensive and compact microwave exposure system that could be accurately calibrated and used for studying effects to small biological specimens at a frequency of 2450 MHz. Following this, platelet-rich human blood plasma was irradiated with microwaves to observe non-thermal effects to platelets and coagulation time as a function of incident power density and absorbed power.

An exposure system was built at a cost of less than $10,000 and requiring less than 11.0 m^2 of laboratory space. The system provides a beam area with a diameter of about one wavelength (12.24 cm) with 3 dB uniformity. It also provides continuous output at any selected power density up to 1.0 W/cm^2.

Investigation of the non-thermal effects to human blood plasma showed that no significant changes occur to <u>in vitro</u> platelets,

coagulation time or clot strength for power densities up to 280 mW/cm^2. This is true for continuous exposure of 0.5 hours to 24 hours.

An unusual observation was noted from microwave heating of the blood above the normal body temperature of 37°C. As the temperature increases from 37°C to 42°C with external application of heat, there is a definite increase in the coagulation time of the blood and a similar but opposite decrease in the clot strength. However, using microwave heating to produce the same temperature results in very little change in both the coagulation time and clot strength. No satisfactory hypothesis has been given to explain this observation and it is suggested that such results be investigated by another independent study.

As a result of this research, it has become apparent that there is a need to continue to investigate other aspects of low-level biological effects, and that there is a need for workers to develop an awareness of the potential hazards associated with microwave equipment. Also, there is an urgent need to develop standardized and more effective measurement techniques and uniformly accepted radiation safety criteria.

CHAPTER I

INTRODUCTION

Background

As early as 1890, D'Arsonval demonstrated that electromagnetic radiation could produce a significant heating effect on humans. Since that time members of the medical profession and others have been investigating the results of, and developing new applications for, this thermal characteristic of electromagnetic waves on matter. One of the early applications used these waves for medical therapy.

As scientific knowledge in this area increased, higher frequencies were being studied so that by 1935, frequencies of up to 10 MHz were being utilized. However, it was not until World War II and the development of a technique called radio detection and ranging (RADAR), which used higher frequencies and much higher power levels, that the problems of biological damage received a significant amount of attention. At this time, man demonstrated the effectiveness of a new portion of the electromagnetic spectrum which is now referred to as the microwave region. While the exact limits are not specifically defined, it is generally accepted to fall into that portion of the spectrum from 300 MHz to 300,000 MHz.

Following World War II, radar systems that were capable of emitting average power levels in excess of one kilowatt were developed. It was noted that the high power densities produced were capable of heating the skin of individuals several hundred feet from the radiating antenna. It was further noted that there appeared to be a unique relationship between

certain frequencies and the depth of penetration which resulted in selective heating in matter.

As a result of these discoveries, many new applications for microwave radiation have been developed. These include drying, thawing, cooking, sterilization, communications, radio-navigation, and tracking. Other applications which are being investigated include: space propulsion, controlled nuclear fusion, microwave ionized gases, microwave motors and microwave controlled helicopters.[1] To show the tremendous growth which has been occurring and which can be anticipated, total sales in 1968 of all types of microwave ovens were projected at about 40,000 units per year and if the price of consumer units were to drop to $250, sales might exceed 500,000 per year.[2]

The potential for biological damage from devices emitting microwave radiation and the possible health hazards was recognized shortly after the development of the military applications of radar. Some of the first studies were conducted by Daily on U.S. Navy personnel employed in the testing and operation of relatively low powered radar.[3] Although this first study produced no evidence of radar-induced pathology in humans, animal studies during the fifteen years following World War II showed that cataracts, corneal opacities, testicular degeneration and hemorrhaging could be produced from exposure to microwaves.[4-6] During this same period, cataracts were first observed in a technician operating a microwave generator.[7]

The medical profession, as well as military and industrial organizations, soon developed an awareness of the potential biological hazards from microwaves. It was recognized that the principal effect

resulted from the heating of tissue. In 1956, a Tri-Service Committee was formed in the United States of representatives from the Army, Navy, and Air Force to investigate the biological hazards and to establish safe levels of exposure for military personnel. As a result of several Tri-Service Conferences which evaluated research conducted with experimental animals and information on human exposures, the Committee proposed an average power density limit of 10 mW/cm^2 as the maximum acceptable continuous exposure limit.[8-11]

This limit was based on two main conclusions: first, it had been theoretically and experimentally determined that continuous whole body exposure of a human to this power density would result in a maximum equilibrium body temperature rise of 1° C--a level considered tolerable on a long term basis without risk to irreversible damage;[12,13] second, several investigations have shown that animals exposed to power densities of approximately 100 mW/cm^2 exhibited irreversible tissue damage. Therefore, by applying a safety factor of 10, the level of 10 mW/cm^2 was proposed. Moore[14] and Schwan[15] have reviewed many of the animal and human investigations which have, in most cases, evaluated the thermal effects of microwave radiation.

While U.S. investigators have, in the past, concentrated a majority of their efforts in looking at thermal effects, studies in the U.S.S.R. have been concerned with functional changes in the cardiovascular and central nervous systems at low power density levels.[16-19] As a result of these investigations, and conclusions regarding low level effects presented in a text by Letavet and Gordon,[20] the Russians have established a microwave radiation standard of 0.01 mW/cm^2 for continuous

exposure, 0.1 mW/cm^2 for exposures of two hours and 1.0 mW/cm^2 for no more than a 20-minute exposure for each work day. It is significant to note that the limit established by the U.S.S.R. is 10^3 lower than the criteria accepted by most U.S. organizations.

It is apparent that many uncertainties still exist regarding the biological effects of microwave radiation, and that much needs to be done toward the development of better instrumentation and dosimetry techniques. Cleary[21] and others have recommended that additional work needs to be done in molecular research, cellular research, and animal experimentation, as well as epidemiological investigations to answer the question of whether the clinical effects reported in the Russian literature can be detected in a study of microwave workers.

Purpose of Research

It was the purpose of this research to:

(1) Design and fabricate the necessary microwave irradiation system required to perform precision measurements and analysis of small biological specimens, and

(2) Study the non-thermal effects to human blood plasma as a function of microwave power levels. The blood parameters studied include platelet count and actual coagulation time as a function of microwave power density, and the dielectric properties of blood plasma.

CHAPTER II

ACTION ON BIOLOGICAL TISSUES

As previously mentioned, the microwave portion of the electromagnetic spectrum is considered to include those frequencies from 300 to 300,000 MHz. This corresponds to wavelengths of 1 meter to 1 millimeter and photon energies of 10^{-6} to 10^{-3} electron Volts. It is apparent, therefore, that the photon energies available are too low to produce ionization such as can be expected from the more familiar ionizing radiation. Excitation is the primary method of energy transfer to biological systems and the transitions between energy levels in the molecular state that can be affected by microwave radiation are the small transitions associated with thermal effects and magnetic orientation.

On striking an object, microwaves may be transmitted through the material, scattered from it, absorbed within it or any combination of these depending on the nature of the material. In the case of biological tissue, determination of the absorbed energy is complicated by many additional factors including inhomogeneity of the target, varying dielectric properties, body mass in relation to the exposed area, and the frequency of the microwave radiation.

The exact nature of the biological effects from microwaves is still being investigated. However, most of the past research has been directed to studying the apparent effects due to general or local heating. Since temperature is related directly to the rate and extent of molecular

vibrations, a large part of the temperature rise is due to the increased vibration of polar molecules.[22] A polar molecule is neutral even though there is an asymmetrical distribution of charge within the molecule, as in the case of water.[23]

In order to increase our understanding of the interaction of electromagnetic radiation with human tissue, it is necessary to know the electrical properties of the body. From an electrical point of view, Schwan[24] broadly classified tissue into the following two groups: tissues of a dielectric constant from 50 to 70 and a specific resistance of about 100 ohm-cm in the frequency range from 100 to 1000 MHz (including muscle and body organ tissues such as liver, kidney, and heart--all having a high water content); and, tissues of a lower water content having a much lower dielectric constant and higher specific resistances (including fatty tissue, bone, and yellow bone marrow). The dielectric constant and specific resistance for tissue decrease slowly as the frequency increases from 100 to 1000 MHz and decrease more rapidly above that value.

In determining the frequencies to be used to study biological effects, it is necessary to realize that the greatest effect to the body occurs at frequencies between about 150 MHz and 3000 MHz. Below 150 MHz, the body is relatively transparent to the radiation and above 3000 MHz, there is more limited penetration below the skin.

Thermal Effects

While it was not the purpose of this research to investigate general thermal effects, it is advisable to briefly comment on some of

the significant work which has been performed, since the radiation protection limits being used in the United States are generally based upon these studies. In addition, several investigators have suggested that separation between strictly thermal and strictly non-thermal effects should not be made.

An excessive increase in body temperature from microwave irradiation produces biological damage which is indistinguishable from fever of other origin. The rate at which heat is dissipated varies considerably, and intermittent exposure is better tolerated by the body than constant exposure at similar power levels.

Some of the first comprehensive studies on the heating effects were performed in 1957 by Ely and Goldman.[25,26] Using a power density of 0.1 W/cm^2, they found lethal fevers in rats, rabbits, and dogs. Also, a comparison of the heating effects to the whole body, eye, and testes indicated that the testes were the most sensitive. There is evidence that moderate damage is probably reversible with a possibility of temporary sterility.

Michaelson *et al.*[27] indicated that rats exposed to 24,500 MHz at 250 mW/cm^2 showed a significant increase in survival time when the environmental temperature was reduced from 35° C to 15° C.

Recent animal studies on thermal effects by Michaelson[28] and others indicate that when death occurs during or at certain periods following exposure, it is impossible to establish a simple relationship between lethality, intensity, duration of exposure and frequency. It depends on a comination of all conditions of irradiation as well as the state of the animal.

Conclusions reached by Susskind from studies of mice, rats, and guinea pigs are: 0.10 W/cm^2 is probably too high to be considered the threshold power density; this value should be lowered to 0.05 to 0.06 W/cm^2; and, it is the body temperature which determines when death will occur, rather than the dose of microwave energy per second.

It is apparent from these and other studies that the thermal effects from microwave radiation are extremely complex. In addition, calculations made in a study by Hoeft[29] indicate that results of experiments performed with rats and mice cannot be used to predict effects on humans unless the differences in size, weight, and exposure times are taken into account.

Based upon the research of thermal effects presented in this section of the report, one should question if it is satisfactory to accept 10 mW/cm^2 as an acceptable power density for continuous human exposure to microwave radiation.

Ocular Effects

The only hazard associated with exposure to microwave radiation environments to occur in man, that has been documented in the United States, is that of microwave-induced cataracts.[30] In 1952, Hirsch[31] reported cataract formation in a laboratory technician whose eyes were exposed in routine daily work to a power density of 0.1 W/cm^2 for approximately one year. Zaret reported in 1967 that 31 documented microwave eye injuries had been reported, and he presented the following evaluation on five of the cases.[32]

> Analysis of these cases revealed that the initial site of pathology was not in the lens substance itself, but, instead,

> in the capsule surrounding the lens at its posterior surface. Ordinarily there occurred a latent period of months to years before the initial pathology appeared. Normally, the lens capsule is transparent, approximately one micron thick and smooth. Careful slit-lamp examination discloses that the microwave injured capsule becomes opaque, thickened and rough. Gradually, this process spreads until the entire posterior capsule and part of the anterior capsule is involved. At this point, which again may take months to years before it appears, the individual may not yet be aware that there is anything abnormal about his eyes because the filtering effect of opacification of the thin lens capsule is minimal and the lens substance, itself, is completely transparent and refracts light normally. Although the process usually takes years to reach this stage of development, the next phase, extensive opacification of the lens substance, occurs rapidly and results in the formation of a clinical cataract associated with a loss of visual acuity.

Microwave-induced cataracts have been produced in a variety of animals,[4,5,30,33-37] and also implied in cataract formation in men following accidental exposure.[38-41]

In 1958 and 1962, Carpenter[39,40] presented evidence that pulsed radar with a high peak power is more effective in cataract production in a rabbit's eye than continuous output of the same power. Conflicting information by Zaret in 1967[30] states that lens changes of rabbits induced by acute exposure to 5400 MHz were found to be directly related to average power irrespective of the wave form, whether continuous or pulsed, and in the latter instance, irrespective of peak power or pulsed duration.

Further research reported by Carpenter and VanUmmersen in 1969[42] indicated that when comparing pulsed vs. continuous wave radiation, the results are inconclusive. Evidence suggests that microwave cataracts are not simply a result of heating but are caused by some other property of the radiation. They report that repeated short exposures can have a cumulative effect, the main determining factor being the time interval

between successive exposures. An interesting observation they reported which can lead to much speculation is that, when irradiating rabbit eyes in a free field at frequencies between 2.45 GHz and 10 GHz, the cataract develops in the posterior part of the lens and resembles a cataract caused by ionizing radiation. However, when the eye is irradiated at the same frequencies as part of a "closed" waveguide system, the cataract develops in the anterior part of the lens and resembles those produced by infrared radiation.

It is worth pointing out here that the analysis of any biological sample in a closed system is extremely complex. Due to the aqueous nature of most samples and the resulting high dielectric constant, it is difficult to determine the exact amount of microwave power which is absorbed by any given incremental sample within the waveguide system.

Non-Thermal Effects

Some of the first studies on the possible non-thermal effects to humans from radiations in the microwave region were performed in the United States in 1945. Lidman and Cohn[43] examined the blood of 124 individuals who had been exposed to microwaves for periods of 2 to 36 months. It was concluded that there was no evidence of stimulation or depression of the erythropoietic or leucocytic systems of these individuals. This is in contrast to more recent studies that are reported later in this chapter.

Following this early investigation, there is an amazing lack of information available concerning effects from chronic or acute low power density exposures. During the same period, however, researchers

in the U.S.S.R. were becoming increasingly aware of subtle effects to the central nervous system and other specific cells and organs of humans and laboratory animals. In 1957, Livshits[44,45] published extensive reviews of studies on the nervous system from exposure to ultra-high frequencies (UHF). As a result of these investigations which began as early as 1934, he concludes that there is a significant effect on the nervous system along with a large rate of action upon the walls of blood vessels, heart muscles, etc. Also, he reports that under the influence of UHF, a significant functional dislocation takes place in all the links of the central and peripheral nervous systems. In many of the reported studies, it is not possible to determine the frequencies or power densities utilized. Using the Atlantic City Convention of 1947, the UHF portion of the electromagnetic spectrum is considered as frequencies of 300 to 3,000 MHz.

In 1962, Presman and Levitina[46] reported on studies with rabbits exposed to power densities of 7 to 12 mW/cm^2 at wavelengths of 12.5 cm (2400 MHz). They noted that during a 20-minute irradiation, and for 10 minutes immediately following, there were changes in the heart rhythm. They stated that irradiation of the ventral parts of the body slowed the heart and irradiation of the dorsal part speeded it. They further suggested that the observed effect was the result of reflex autonomic reactions provoked by the direct action of the microwaves on the superficial reflexogenous zones and the effect from irradiation of the head was produced by action on brain cells.

As was mentioned in Chapter I, the Russian maximum power density allowed for continuous human exposure to microwave radiation is 1000 times

lower than the generally accepted guidelines used in this country. The lower Russian level is based upon the findings of Letavet and Gordon.[47] This study was on clinical observations of 525 microwave workers who had worked in various environments where low-level chronic exposure was likely. Few, if any, had been chronically exposed to levels higher than a few mW/cm^2. Of these 525, 33 per cent showed thyroid enlargement compared with 14 per cent in a control group of 100; bradycardia (or a slowing of the heart action) showed 43 per cent vs. 3 per cent for the control group; headache and increased fatigue, 29 per cent vs. 8-10 per cent; and arterial hypotension, 28 per cent compared to 14 per cent.

An article in 1964 by Kamenskiy[48] adds additional information to support other Russian investigations. Irradiation of the frog nerve at a wavelength of 12.5 cm and a power density of 11 mW/cm^2 for 20 to 30 minutes increased the rate of conduction, shortened the absolute and relative refractory phases and altered the magnitude of the amplitude of action-currents, but had no effect on the excitability threshold. Irradiation of the frog nerve with pulsed microwave (10 cm wavelength, 1 microsecond pulse, 700 pulses/second, 12 mW/cm^2) for 20 to 30 minutes increased the conduction rate and excitability of the nerve. Kamenskiy, as other authors, concludes that the effect of pulsed microwaves can be considered non-thermal (specific), whereas changes observed during non-pulsed radiation might equally well be attributed to a thermal effect. Excellent reviews and translations of Soviet literature can be obtained from the Library of Congress.[49,50]

A study in the United States by Eakin and Thompson[51] on rats exposed to low intensity, low frequency (300 MHz to 920 MHz) UHF radio

waves for 47 consecutive days showed that radiated rats were more active than non-radiated rats during the early part of the experiment and became less active as the days of radiation increased. No differences were found for weight, audiogenic seizures or water consumption. The authors suggest that some time is required for UHF to have a consistent effect on behavior and the effects on behavior may be non-thermal and related to neurophysiological substrates. Behavioral changes have also been noted on experiments using chickens and pulsed microwaves at 9300 MHz and average power densities of 46 mW/cm^2.[52]

Studies have been conducted to evaluate effects to the hematologic system. Most of this work has been based upon whole body irradiation of animals. Results of exposures of dogs and rats to 24,000 MHz indicated that exposure to 10 mW/cm^2 produced temporary hemopoietic effects while exposure to 20 mW/cm^2 was responsible for temporary loss of body weight.[53]

Studies at the University of Rochester indicate that whole body exposure of normal dogs results in leukocyte changes which can be related to frequency, field intensity, and duration of exposure.[28,54] Early and sustained leukocytosis in dogs exposed to microwaves may be related to stimulation of the hematopoietic system or recirculation of sequestered cells.

A decrease in erythrocyte, leukocyte and hemoglobin values has been noted during irradiation of mice at 10,000 MHz and 450 mW/cm^2 for five minutes.[55] Such a decrease was noted immediately after exposure and at one and five days. Hematologic recovery was noted at 10 days post irradiation. Conventional heating produced less distinct changes, with more rapid recovery than exposure to microwaves.

In 1965, Sigler et al.[56] completed a statistical study of the radiation exposure history of the parents of 216 Mongols. One of the statistically significant results of this study was data showing an increased incidence of Mongol births where there was a paternal microwave radar exposure history. This observation was not anticipated as a part of the study and, as a result, additional follow-up surveys are now being conducted at the Johns Hopkins Hospital to further evaluate this discovery.

It is apparent that much valuable information has been obtained from studies on the low-level or non-thermal effects produced at various frequencies and power densities of microwave radiation. However, it is also obvious that much more needs to be done to study the effects on biological systems and that such data is urgently needed in order to adequately determine safe exposure limits for humans.

Synergistic Effect with X-Rays

Several studies in both the Unites States and the U.S.S.R. have been conducted to observe the effect of combined X-ray and microwave irradiation on animals. Loshak[57] utilizied pulsed UHF radiation at 1.0 mW/cm^2 and ionizing radiation (180 kV X-rays, 900 R whole body exposure). The results did not show that preliminary microwave irradiation had any protective effect. He found that pre-UHF exposure actually resulted in a more rapid mortality of X-ray irradiated animals. He attributed the results to the effects of UHF on hematopoietic structures, which implies that these organs are even more sensitive to UHF radiation than neural structures. He stated that the lifespans of the animals indicated hematopoietic injury (especially of the bone marrow).

In contrast to these findings, Michaelson[54] summarized other studies which tend to conflict, or at least raise additional questions, with those noted above. Dogs receiving whole body microwave irradiation showed significant increase in survival time when exposed to 25,000 R, 1000 kVp X-rays to the head. Mortality after whole body irradiation with 1000 kVp X-rays is substantially lower among dogs previously receiving microwave exposures. Simultaneous exposure to pulsed 2800 MHz, 100 mW/cm^2 microwaves and 250 kVp X-rays, 720 R (2 R/min), results in earlier leukocyte recovery from radiation-induced leukopenia. However, such earlier recovery is not observed at a higher exposure rate of 4.6 R/min.[58,59] In rats that received 2500 MHz continuous, 10 mW/cm^2, 30-minute exposures for 25 days, mortality from subsequent gamma-irradiation (600 R) is one-third that in the controls, whereas irradiation with pulsed microwaves under similar conditions produced no effect.[60]

The noted changes in response to X-ray exposure are related to the length and sequence of the microwave exposures as well as the time interval between the microwave exposure and the X-irradiation. Except for increase in survival time and less severe neurologic response in microwave-treated dogs receiving X-irradiation to the head, modification of the X-ray injury has most demonstrable effect on the hematopoietic system.[28,61-63]

From this review of the literature, it is apparent that much has been learned on the biological effects from microwave radiation. Our knowledge has increased but much remains to be learned. Because of the variables and uncertainties which have been described, it is felt that there is still a lack of adequate data to establish an absolute safe

level for exposure to radiation in the microwave region of the electromagnetic spectrum.

It is very apparent that it is difficult to reach specific conclusions since results vary widely among the studies noted in the literature. The problem is compounded by the fact that the reports often fail to present enough information to allow for an effective evaluation of the results. But of more importance, is the difficulty in developing techniques for generating uniform fields and plane waves in a carefully controlled environment. It was the purpose of this research to design a system in which the frequency, power, exposure and wave characteristics are precisely determined and controlled. With the use of this system, research was performed that is an extension of studies by Lamb[64] and Richardson.[65]

CHAPTER III

INSTRUMENTATION AND EQUIPMENT

The experimental apparatus is designed to allow for the microwave irradiation of relatively small biological samples at a frequency of 2450 MHz under precisely known power densities at any of a wide range of power levels. The 2450 MHz frequency was selected because of the recent rapid introduction of commercial applications utilizing this frequency and the need for additional research to investigate the biological effects resulting from accurately known levels of exposure to such frequencies.

Few researchers have the financial resources or time to fabricate a high power microwave system in an elaborate and expensive anechoic chamber which would enable such biological experiments to be performed in the conventional far-field region of an antenna where accurate power density measurements can be made. It is the purpose of the chapter to describe the technique which was developed to fulfill an objective of design and fabrication of an appropriate microwave exposure system that (1) can be utilized in a limited physical space, (2) is economically feasible, and (3) maintains the far-field characteristics of irradiating samples approximately uniformly and being accurately measurable.

The entire system can be divided into the following separate sections: source and power supply; transmission line; power density control; illuminator; sample support structure; and shielding

and absorber. The complete system can be seen in Figure 1. Figure 2 is a block diagram of the system.

Source and Power Supply

It was determined that the system should have available a minimum power density of up to 100 mW/cm^2. This power density exceeds the present United States accepted level for continuous exposure by 10 dB and the U.S.S.R. maximum recommended level by 40 dB. (In addition, a recent Federal standard states that microwave cooking ovens manufactured after October 6, 1971, may not emit radiation in excess of 1.0 mW/cm^2 prior to oven sales and not more than 5.0 mW/cm^2 throughout the useful life of the oven.) The design should also allow for a maximum power density variation not to exceed 3 dB over a surface with a diameter of approximately one wavelength, or in this case, 12.24 cm.

A Litton L-5001 continuous wave 2450 MHz magnetron was selected since it is well known that this frequency produces maximum effects on biological systems, and this magnetron appeared to be one of the most economical sources of 2450 MHz power. It has a rated output of 1.3 kW, an input voltage of 3.5 kV, and input current of 0.550 A. It is air-cooled, and its rated efficiency is given by the manufacturer as 68%. Such continuous wave magnetrons are frequently used in commercial and domestic microwave ovens and industrial drying ovens.

Transmission Line

The transmission system that carries the source energy to the antenna feed serves as the primary means of determining the power density at the sample. It also contains a sampling point to measure

Figure 1. Complete Microwave Exposure System

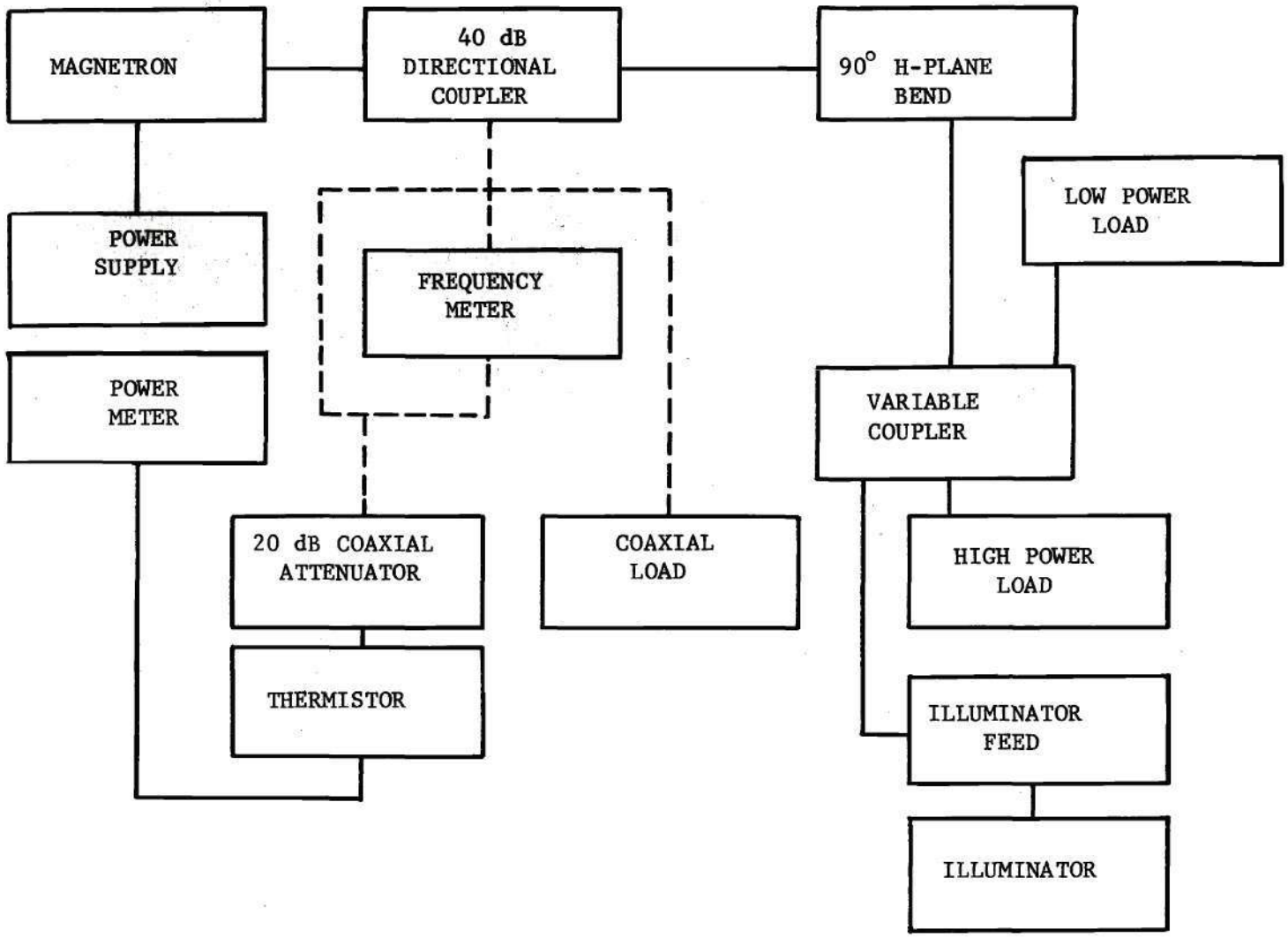

Figure 2. Block Diagram of Microwave Exposure System

frequency and power to the antenna feed. Because of the high power of the source and the frequency involved, it is advisable to use waveguide rather than coaxial line. If waveguide tables are consulted, the recommended size for 2.45 GHz is 4.32 cm x 8.64 cm, which is known as WR 340. However, components are less expensive and more available in WR 284, commonly known as S-band waveguide, which has inside dimensions of 3.40 cm x 7.21 cm and has a nominal operating range of 2.60 to 3.95 GHz. The cut-off frequency of WR 284 is 2.08 GHz; therefore, 2.45 GHz is still above cut-off.

Microwave power generated by the magnetron flows through a narrow wall 40 dB directional coupler with a rotary vane attenuator and coaxial output connected to the sidearm. For a source power of 1.0 kW, approximately 100 mW is coupled through the sidearm and attenuator into the coaxial sample port.

At this sample port, it is possible (1) to determine the output frequency through the use of a coaxial-mounted frequency meter, or (2) to monitor the output power of a thermistor mount/power meter combination. Experimental determinations taken from this coaxial sample port are described later in this chapter.

A 90° H-plane bend is connected to the main arm of the 40 dB coupler to allow for a change in direction.

Power Density Control

Connected to the H-plane bend is a variable directional coupler which is a highly specialized microwave circuit providing continuous variation of microwave power by permitting a shifting of output power between two separate and distinct outputs. This device, designed on

the basis of results published by Teeter and Bushore[66] at X-band, produces variable power division by controlling the phase of one-half of the incoming energy relative to the other. A schematic diagram of the power divider is shown in Figure 3 and its location in the completed system is pictured in Figure 4.

The device was fabricated from two short-slot hybrids with a continuously variable phase shifter (tandem short-circuit with another short-slot hybrid) located between the input and output hybrids. This results in a four-port device which consists of an input port, and output port, and two terminated ports, one beside the input and one beside the output. The terminated input port utilizes a low-power load since it receives only reflected and leakage power which is reduced by at least 30-40 dB from the source power. The terminated output port absorbs up to the full input power and is terminated in a high-power load.

The input power is divided equally by the input hybrid and produces a 90° phase relationship between the straight section and that directed through the intermediate hybrid section. Moving the tandem short-circuit varies the phase relationships of the power arriving at the output hybrid which, in turn, determines the ratio of the power coupled to the output and the high-power load.

When the straight section and tandem short-circuit section are the same electrical length, or if the difference is an exact multiple of the guide wavelength, the power from each section is added and proceeds to the output. As the tandem short-circuit length is changed by a difference of one-fourth guide wavelength, the phase relationship

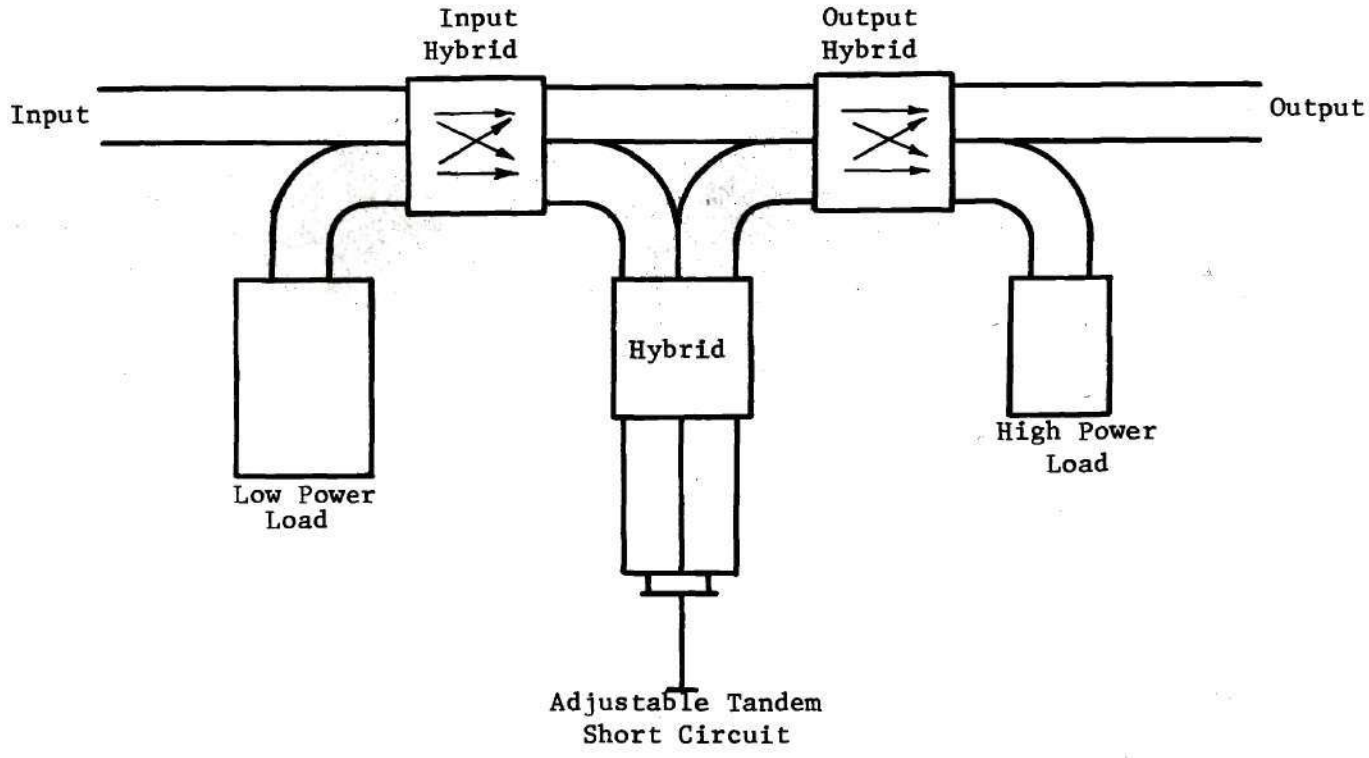

Figure 3. Power Divider System

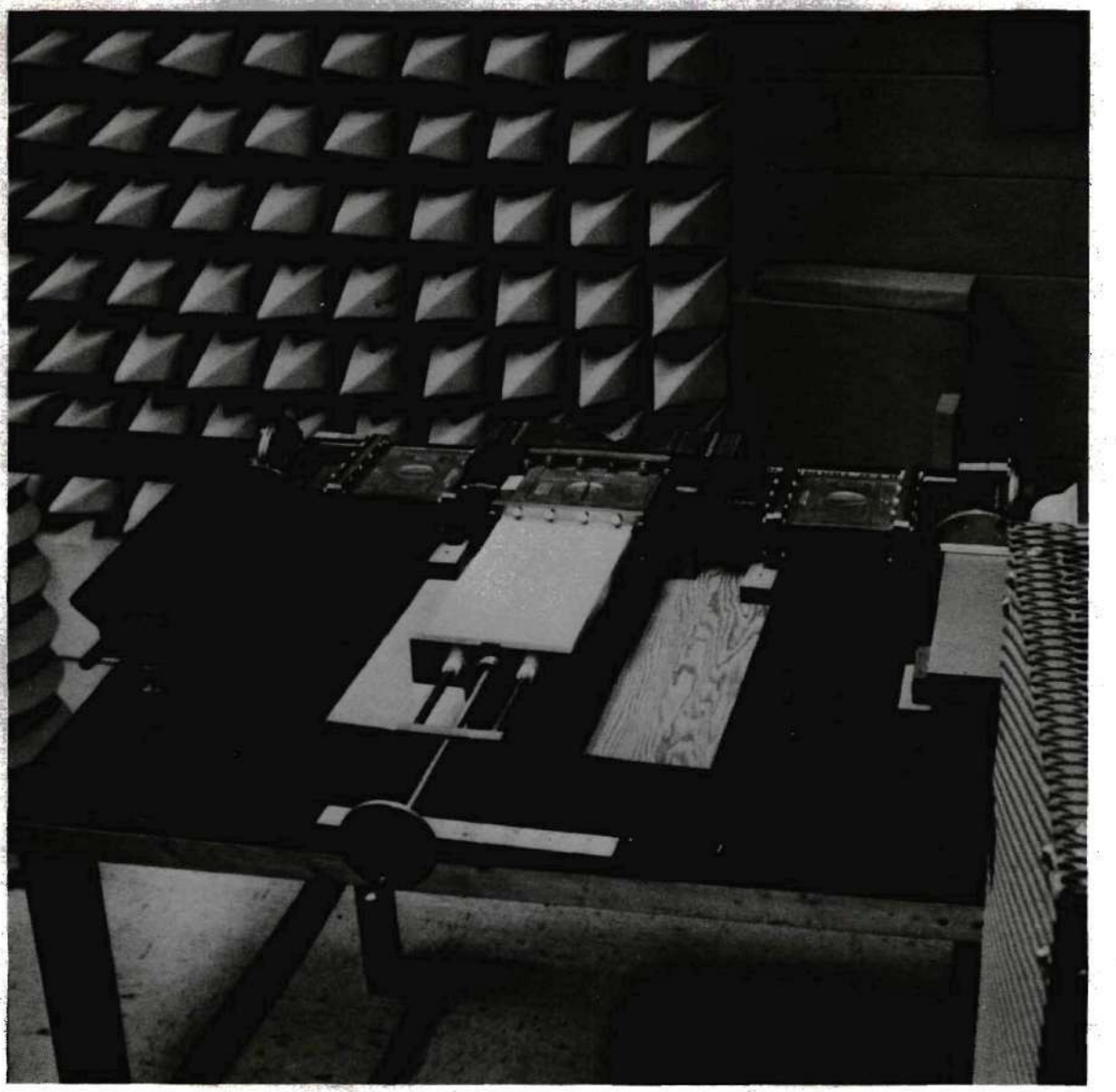

Figure 4. Power Density Control Section

at the output hybrid is such that an equal amount of power appears at the output and the high-power load. When the length is changed by one-half guide wavelength, all power proceeds to the high-power load. As the length changes by three-fourths guide wavelength, the power is again equally divided between the output and the high-power load.

Experimental analysis of the variation in output power was performed. The relative power vs. change in length of the tandem short-circuit was determined and is shown in Figure 5.

VSWR measurements of the complete power divider section were made as the short-circuit length was varied and it was determined that the maximum VSWR (Voltage Standing Wave Ratio) was 1.21.

An unsupported, choked antenna feed was fabricated and attached to the output of the power divider section.

Illuminator

First, one should consider the effect of using a conventional antenna operating as the microwave illuminator. In order to avoid the use of an anechoic chamber, it is necessary to use a relatively narrow beam. Assume that a 50 cm diameter parabola is used at 2450 MHz. The maximum half-power beam width can be determined by:

$$\text{half-power width} = \frac{70\lambda}{D} \text{ degrees} \quad [67] \qquad (1)$$

where: λ = free-space wavelength

D = antenna diameter

half-power width = approximately 17°

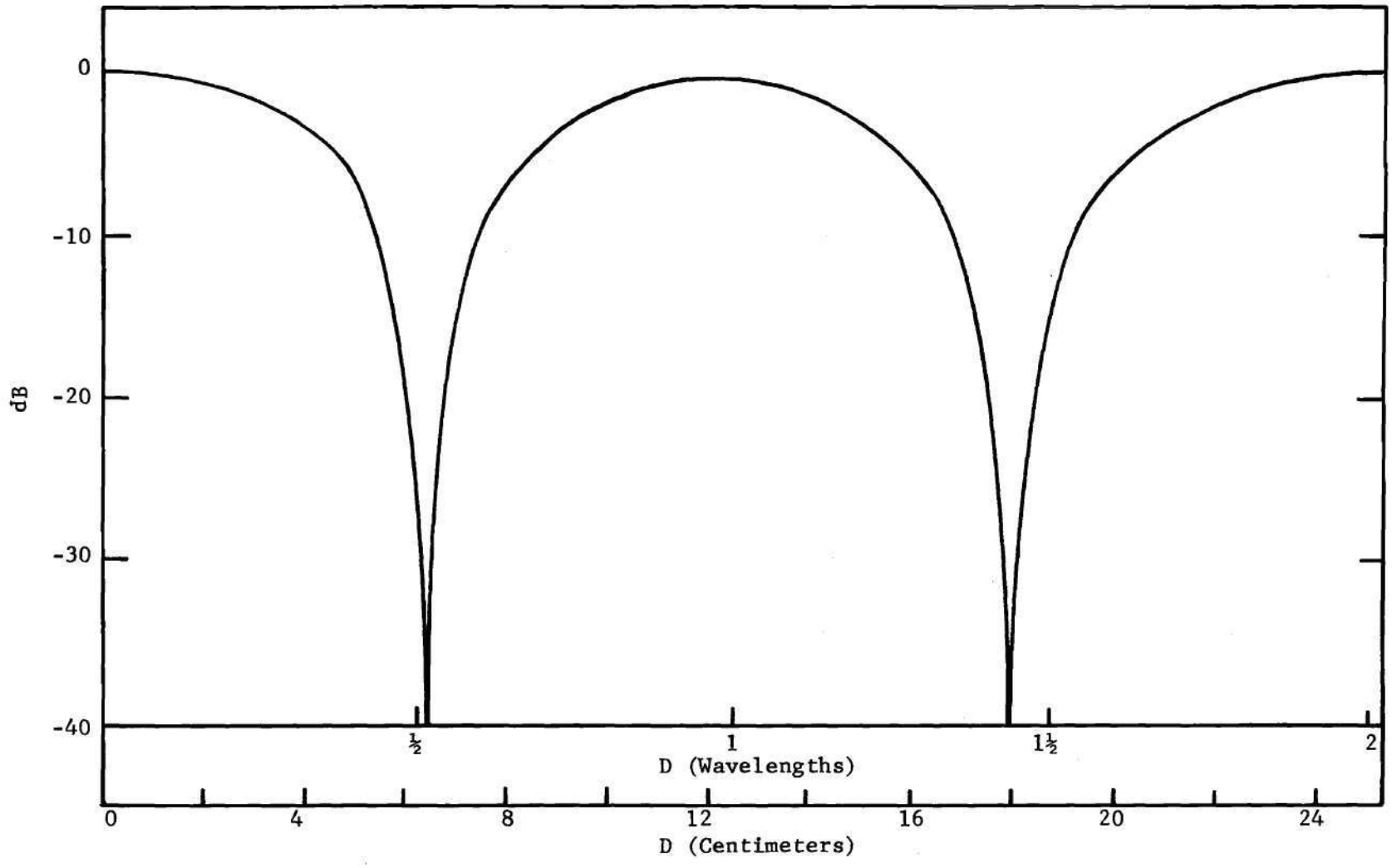

Figure 5. Relative Power, in dB, vs. Change in Length, D, of Tandem Short Circuits

A distance of at least 4.1 meters is needed to get into the far field region of $2D^2/\lambda$. It is apparent that a relatively large room would be required for such a microwave system. The approximate area irradiated at this minimum distance is 12,000 cm^2. Using the criteria noted earlier for specifying source power, it can be seen that a source of several thousand Watts would be required to achieve a power density of 100 mW/cm^2.

The illuminator used in this research is a 1.17 meter diameter focused prolate-spheroid antenna which makes it possible to avoid the space and power problems that have been mentioned with a typical illuminator. This focused system utilizes a reflector which has two foci, as shown in Figure 6. It is illuminated by the choked open-ended waveguide at the inner focus which has been shown to be one of the most effective feeds by Bassett and Bomar.[68] The irradiated sample is positioned at the outer focus.

The inherent advantage to the focused system, as compared to the other systems using the same size reflectors, is that less antenna input power is required to establish a given power density. As observed by Primich and Hayami[69] and later by Bassett and Bomar, the focal region wavefront is uniform (within 3 dB) over a diameter of up to 1.5λ, which is much greater than the sample sizes utilized in this study and described in the next chapter.

The minimum spot size can be related to the focal length and diameter of the reflector by the following relation:[70]

$$1.22\ f/D = \rho/\lambda \qquad (2)$$

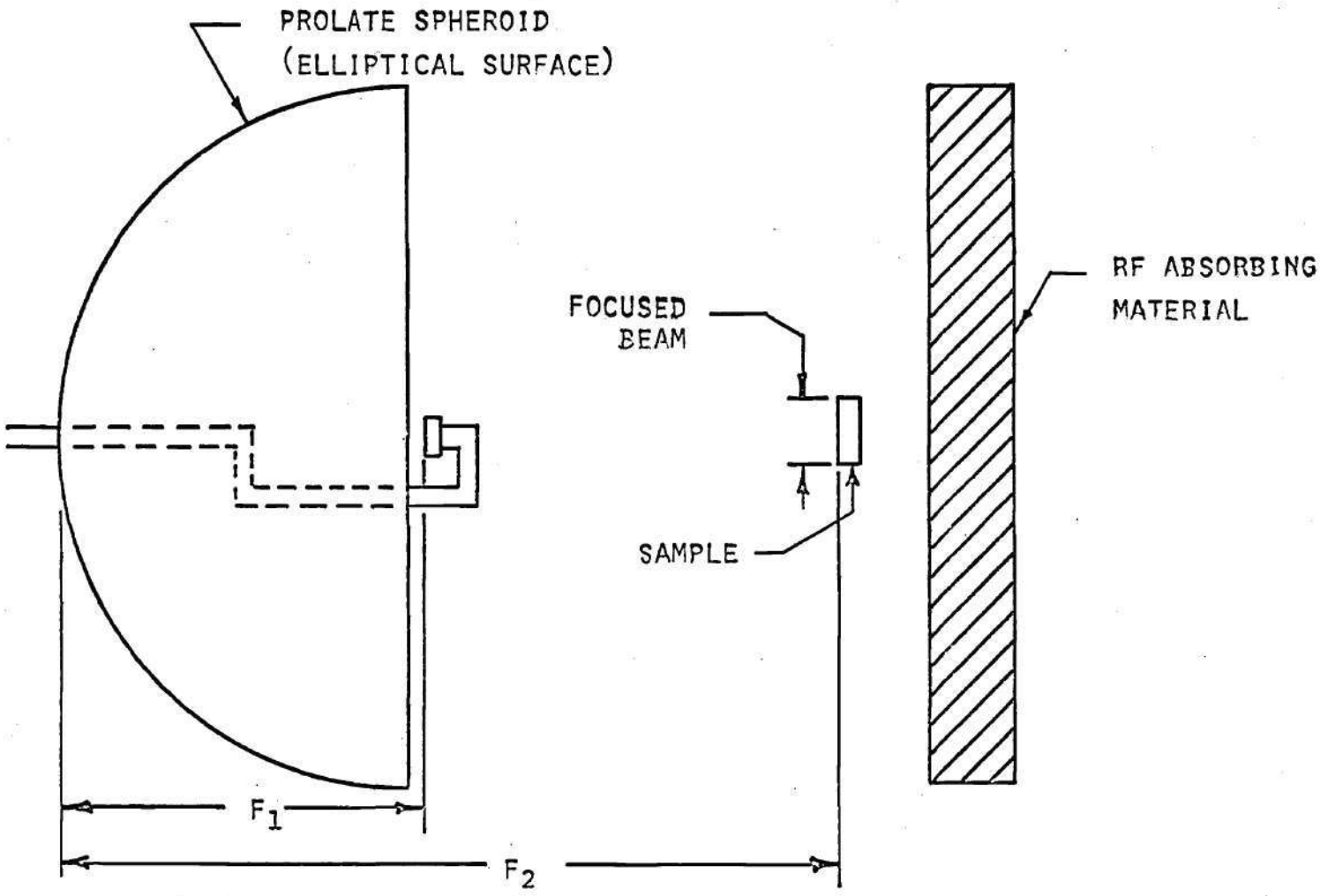

Figure 6. Diagram of Focused Prolate Spheroid Illumination System

where:

f = focal length

D = reflector diameter

λ = free-space wavelength

ρ = diameter of spot at focal point

It is noted from equation (2) that the spot size can be increased by increasing the ratio, f/D. To be practical, this means that the diameter of the reflector should be decreased significantly. This diameter decrease involves a change in the feed-horn illumination which would result in a very inefficient system. Reflector edge spill-over would be significant, and the focused beam properties are not readily predictable.

The conclusion drawn from the investigation of the utility of using the focused beam system is, that for radiation of small samples whose dimensions are on the order of a radiation wavelength, the system is very efficient.

For the purpose of these investigations, the midline of the antenna and focal points was 105 cm above the floor. The first focal point (located at the choked antenna feed) was a distance of 43.2 cm from the center point of the antenna. A longitudinal profile of the second (sample) focal point was made and the relative power vs. distance is shown in Figure 7. The center of this second focus was determined to be 61 cm in front of the first focal point.

Figures 8 and 9 show the E-plane and H-plane profile patterns through the second focus. It can be seen that an area with a diameter of approximately 6 cm (about ½ wavelength) can be irradiated with 1 dB

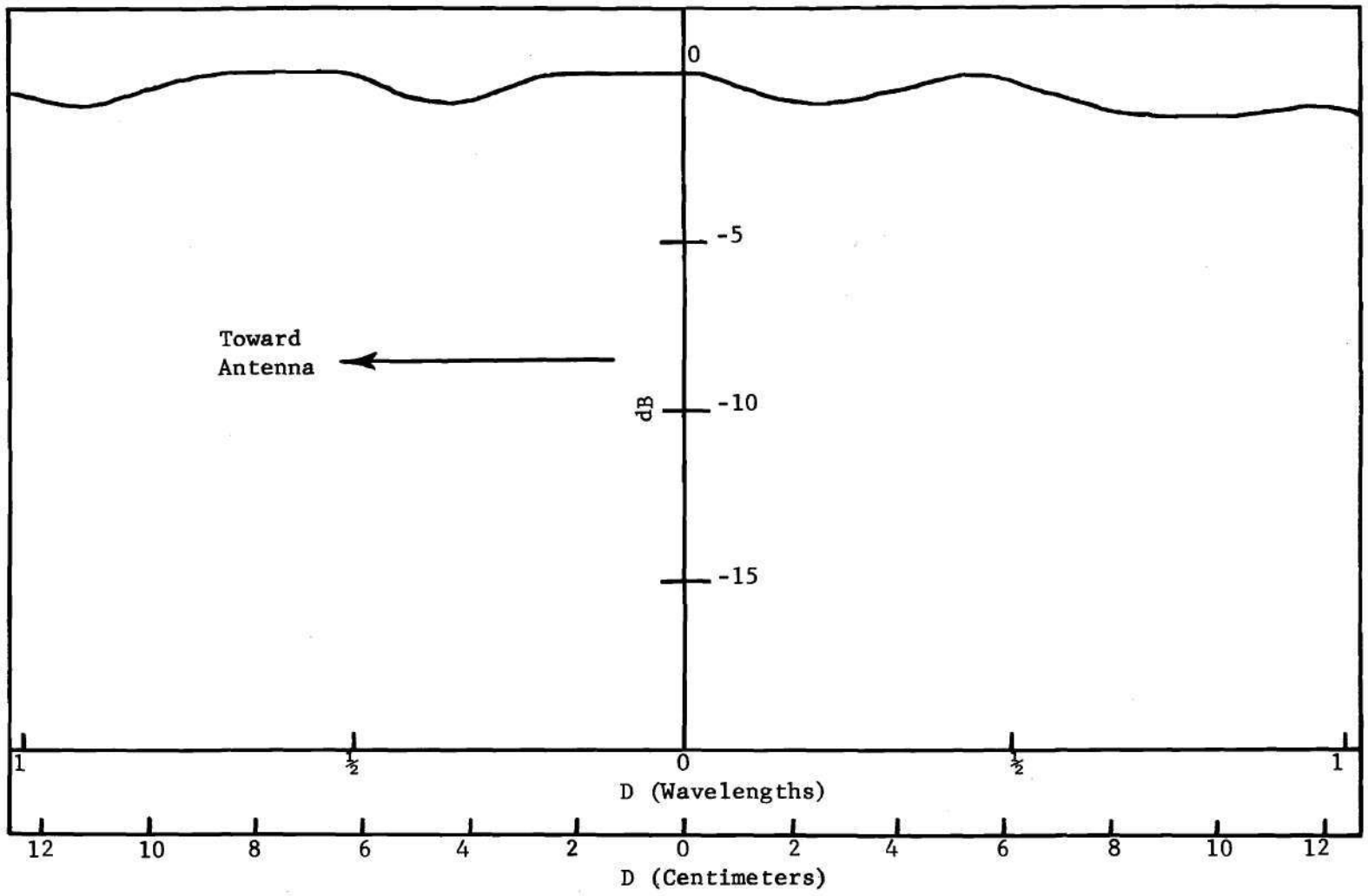

Figure 7. Longitudinal Profile of Second Focal Point in Relative Power, in dB, vs. Distance, D

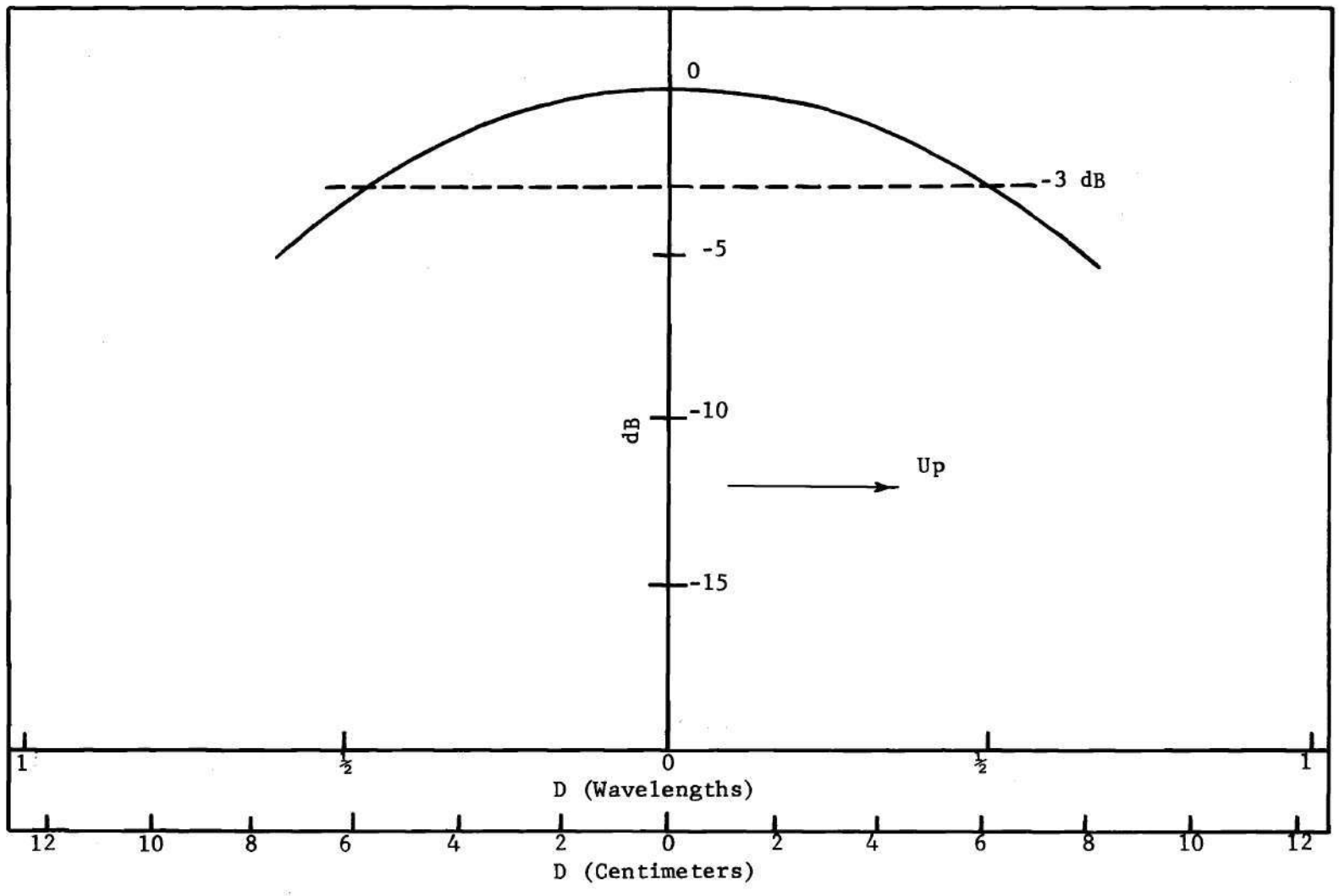

Figure 8. E-Plane Profile of Relative Power, in dB, vs. Distance, D, from Longitudinal Axis for the Second Focal Point

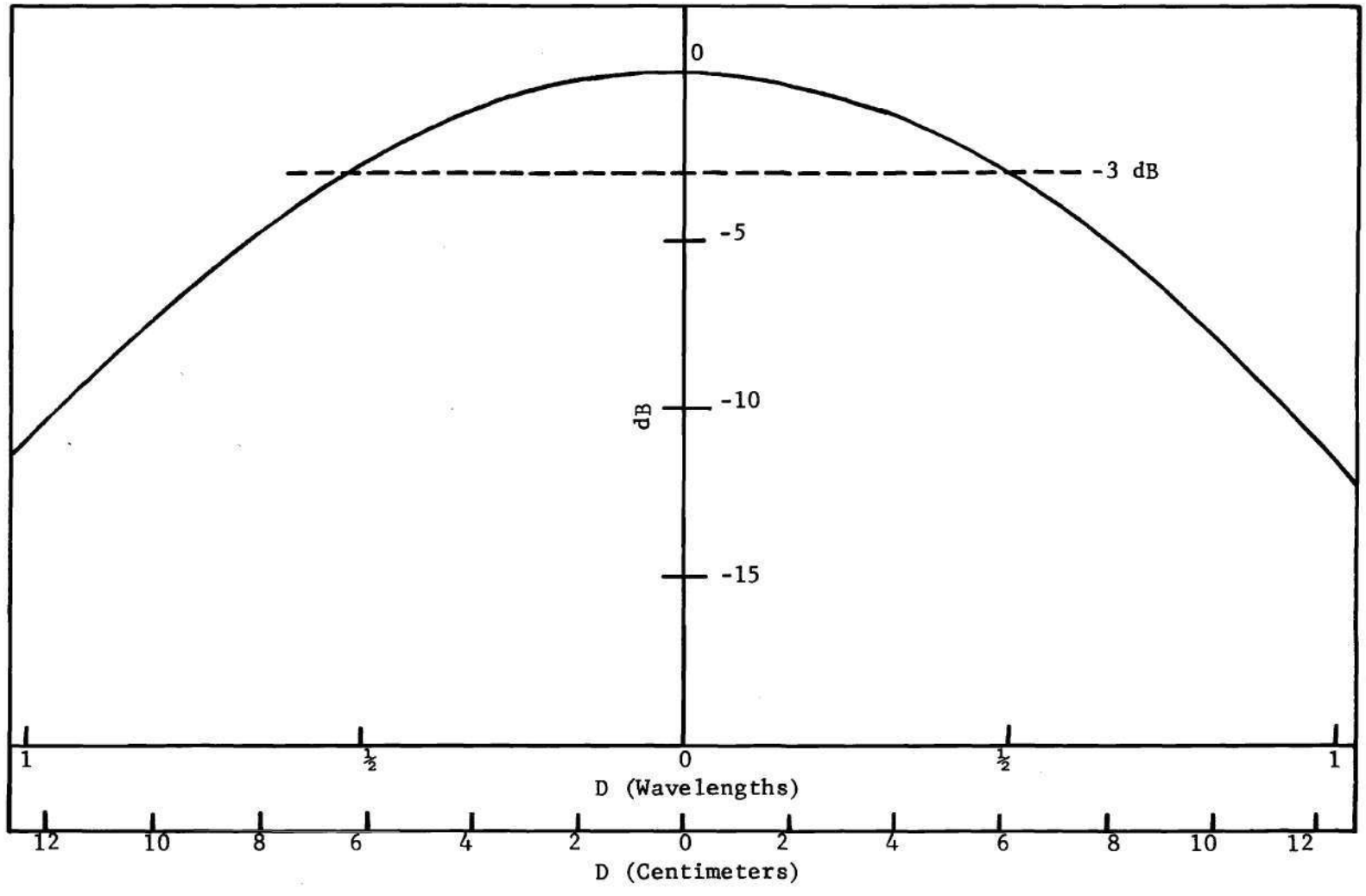

Figure 9. H-Plane Profile of Relative Power, in dB, vs. Distance, D, from Longitudinal Axis for the Second Focal Point

uniformity and an area with a diameter of approximately 12 cm (about 1 wavelength) can be irradiated within 3 dB uniformity.

Sample Support Structure

The sample had to be supported within the microwave beam by a structure that would not cause interference with the incident radiation field. A specially designed cellular plastic column of varying dimensions was fabricated in order to (1) minimize reflections and backscatter, (2) be relatively transparent to the microwaves, and (3) provide the necessary rigid support. The structure utilized a series of cellular, low-dielectric ($\epsilon_r \sim 1.03$) disks of 10.15 cm thickness varying in diameter from 15.2 cm to 61.0 cm. The edges of each disk were beveled at an angle of 60° to the horizontal so as to provide diffuse scattering. Senior, Plonus and Knott[71] have shown structures of this type to have a measured incoherent cross section of $-53.2\ dBm^2$ at X-band.

Shielding and Absorber Requirements

The system as previously described makes it possible to design and install a simple absorbing panel which can be utilized with little or no sacrifice in safety and performance as compared with the much more expensive anechoic chamber. This is possible since it has been shown that the power is focused to approximately a 12 cm spot size and that very little divergence of the beam occurs within 3 meters of the antenna. A $4.46\ m^2$ mobile absorbing panel with dimensions greater than twice that of the antenna aperture was fabricated using commercially available microwave absorbing material. This mobile panel was placed behind the sample holder and centered about a longitudinal axis

running through the center of the antenna. According to the manufacturer's specifications, the absorber has a reflectivity of -40 dB at 2450 MHz. Therefore, microwave energy not absorbed by the test sample would, at a maximum power density of 100 mW/cm^2, be at a level of 0.01 mW/cm^2 after being reflected from the mobile absorbing panel. In addition, this panel would not allow any significant reflected energy to interact with the test specimens since it will always be at least 40 dB below the incident test level.

No other absorbing material was necessary. However, precautions were taken to prevent the introduction of other material in the immediate area of maximum power. Even though later studies indicated that the maximum power density at the second focal point exceeded expectations, the shielding as described proved to be more than adequate.

Maximum Power Density

It was the purpose of this research to design and build a microwave exposure system that could adequately irradiate small biological samples to power densities up to a minimum of 100 mW/cm^2. However, it was advisable to determine for safety reasons the maximum power output that was available. This maximum power density was determined experimentally to be about 1 W/cm^2. This level was confirmed using the power divider output curves as previously shown in Figure 5.

Maximum Power Output

Measurement of high power outputs such as that expected in determining the maximum output of this system generally relies on the use of calorimetric techniques since appreciable heat is developed by

the dissipation of Watts of power. The water load, most widely used detector for high-level microwave power measurements, relies on the calorimetric principle. The power is totally absorbed in a matched-impedance section of waveguide which contains a calibrated flowing stream of water. The water dissipates the power and the resulting rise in temperature is measured with calibrated thermocouples. The temperature rise can then be related to the absolute power level.

The thermistor is one of the most common detectors used in measurement of low- and medium-level powers. It consists of a small resistive element capable of dissipating the power and using the heat developed to produce a change in its resistance. This resistance change is usually measured by using the thermistor as one arm of a Wheatstone-bridge circuit.

In order to use the thermistor for higher power measurements, it is essential that a known ratio of power be diverted through the use of calibrated directional couplers or similar attenuation to prevent burn-out of the thermistor.

The maximum power output to the antenna from this system was determined to be 250 Watts when the magnetron was operated at a routine input current of 0.3 Amperes and voltage of 3,000 Volts. This was checked and verified by the following procedure. Through the use of a 1000 Hz modulated 2450 MHz signal, a VSWR meter and a E-H tuner - sliding short combination, a commercially available narrow wall 40 dB directional coupler was accurately calibrated and found to couple off 35 dB at the 2450 MHz frequency. To the side arm was attached an additional 15 dB of attenuation. This provided adequate attenuation

to allow the attachment of a thermistor mount and a thermistor/power meter connection.

After removing the antenna and choked feed from the system, this directional coupler combination was connected to the output of the power divider. To the forward end of the main arm of the directional coupler was attached a calibrated water load. The temperature difference between the inlet and outlet water lines was monitored with a thermocouple which was connected to a visual indicator calibrated by the manufacturer. The complete set-up for determining the maximum power output can be seen in Figure 10.

Determinations were made with calibrated water flow rates of 6.3 cc/sec. and 0.934 cc/sec. At each flow rate, the maximum power output was found to be 250 Watts.

Observation with the power meter indicated 54 dBm, or a comparative power output of 251 Watts.

VSWR measurements were made on all items used in these determinations to insure that reflections within the system were minimal.

Power Density Determination

Power density determinations used in the exposure of the biological samples, as well as general safety hazard analysis, were performed using a commercially available portable instrument. This instrument is a direct reading device calibrated for the 2450 MHz frequency and includes three non-polarized hand-held probes, each incorporating a small dipole antenna and detector. The three probes together allow for full-scale readings of from 0.2 mW/cm^2 to 200 mW/cm^2. The manufacturer's specifications indicate an accuracy of ± 1 dB at 2450 MHz.

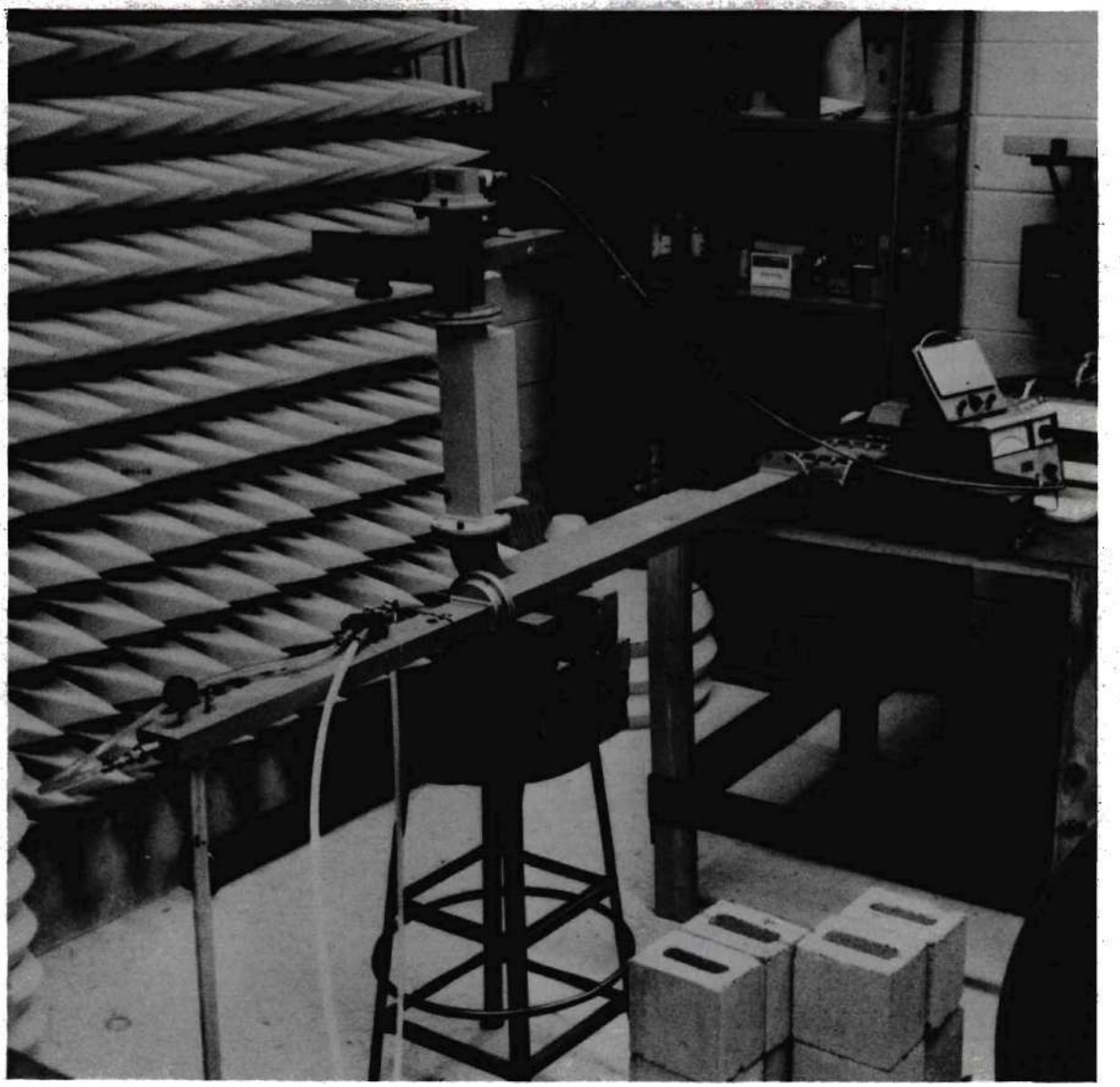

Figure 10. Set-up for Determining the Maximum Power Output

Calibration of Power Density Instrumentation

Although an accuracy of ±1 dB was given by the manufacturer of the above mentioned portable instrument, it was felt advisable to perform an additional evaluation using the microwave system fabricated for this research. The following procedure was used in modifying the system to allow for comparing observed power density levels with calculated values as shown below.

The system as described earlier for determining the maximum power output was modified slightly by removing the water load and replacing it with a pyramidal horn with aperture dimensions of 32.067 cm by 26.035 cm, and having a VSWR of 1.15.

Calculation of the antenna gain was made using procedures described in the Antenna Engineering Handbook.[72]

The gain in dB is

$$G_{dB} = 10(1.008 + \log \frac{a}{\lambda} \frac{b}{\lambda}) - (L_e + L_h) \qquad (3)$$

where:

a = H-plane length = 32.067 cm

b = E-plane length = 26.035 cm

λ = free-space wavelength = 12.24 cm

L_e and L_h are taken from Figures 11 and 12.

To determine L_e from Figure 11, it is seen that

$$s = \frac{b^2}{8\lambda \ell_e} \qquad (4)$$

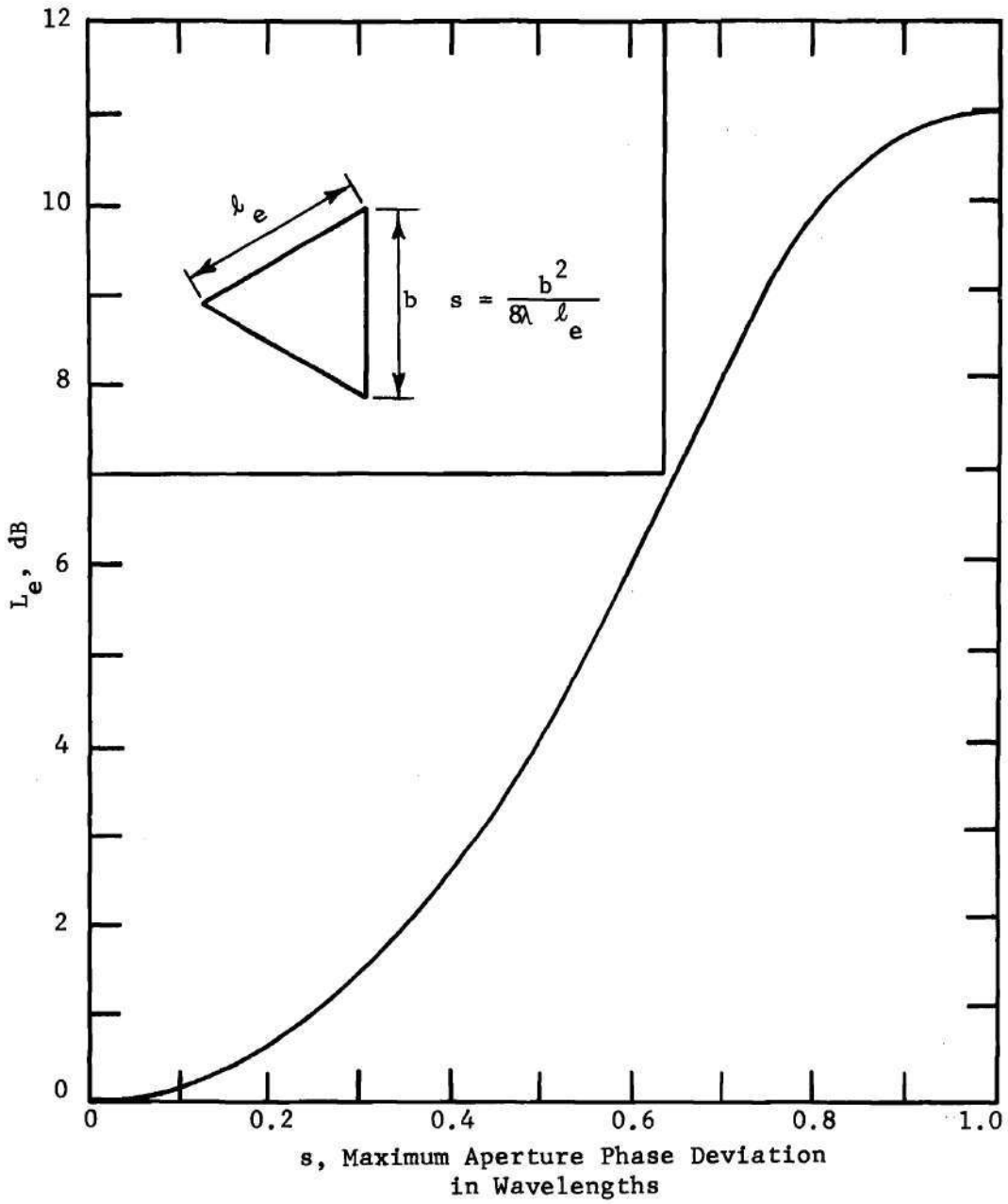

Figure 11. Gain-correction Factor for E-Plane Flare[72]

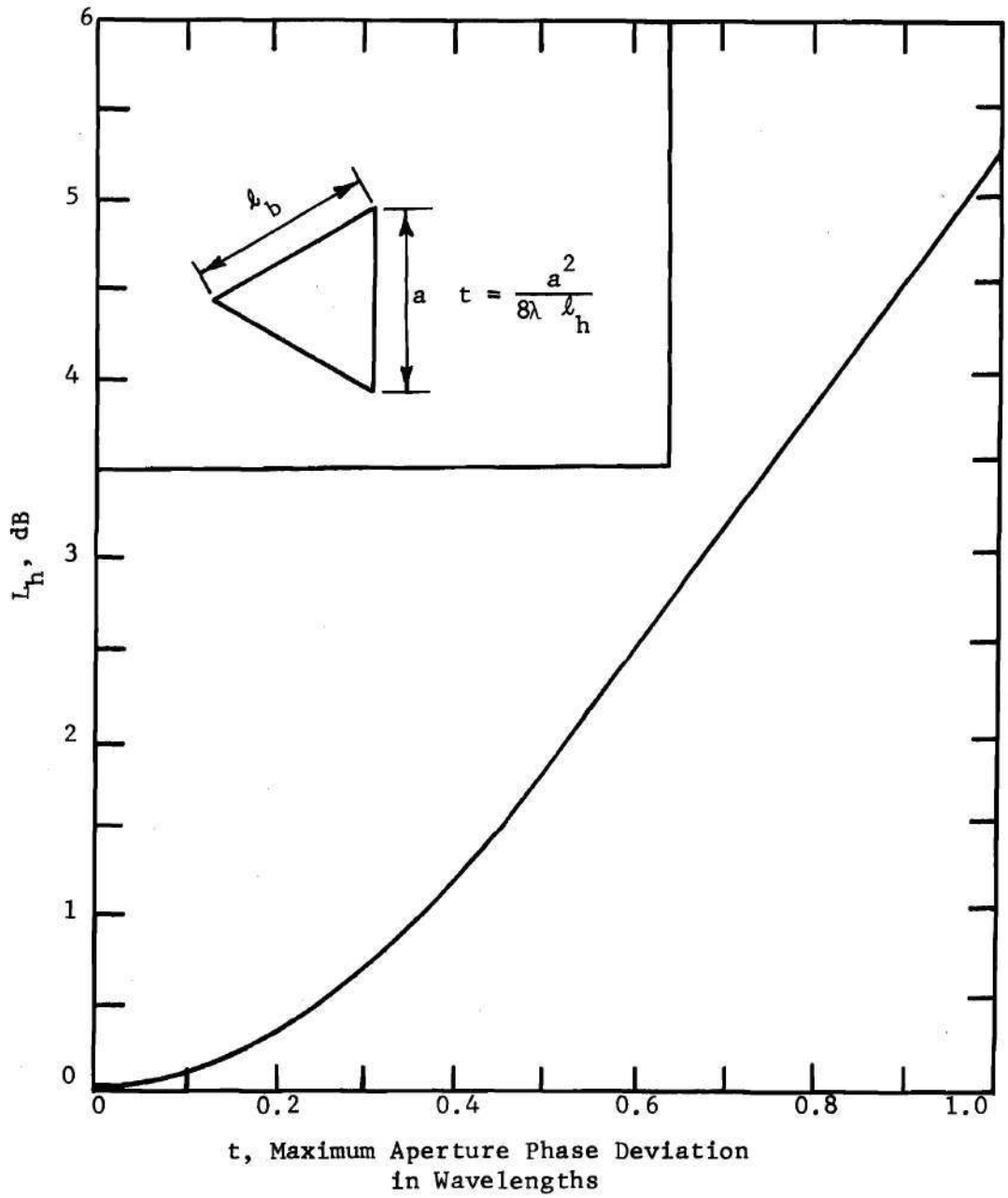

Figure 12. Gain-correction Factor for H-Plane Flare[72]

where:

$$\ell_e = 42.23 \text{ cm}$$

$$s = \frac{(26.035)^2}{8(12.24)(42.23)}$$

$$s = 0.1637$$

Therefore: $L_e = 0.3$ dB.

To determine L_h from Figure 12,

$$t = \frac{a^2}{8\lambda\, \ell_h} \tag{5}$$

where:

$$\ell_h = 47.31 \text{ cm}$$

$$t = \frac{(32.067)^2}{8(12.24)(47.31)}$$

$$t = 0.22$$

Therefore: $L_h = 0.7$ dB

From equation (3):

$$G_{dB} = 10[1.008 + \log (\frac{32.067}{12.24} \cdot \frac{26.035}{12.24})] - (0.3 + 0.7)$$

$$= 10(1.008 + \log 5.563) - 1.0$$

$$= 10(1.008 + 0.7453) - 1.0$$

$$= 10(1.7533) - 1.0$$

$$= 17.533 - 1.0$$

$$G_{dB} = 16.5 \quad \text{or}$$

$$G = \text{antilog } \frac{16.533}{10}$$

$$= 45.0$$

The power density, P_D, from a radiating antenna,

$$P_D = \frac{P_t G}{4\pi(R)^2} \tag{6}$$

where:

P_t = power to antenna

R = distance from antenna

G = antenna gain

The beam is characterized by a near field and a far field, where for a circular antenna the far field is considered as a distance beyond $\frac{2(D)^2}{\lambda}$ where D is the largest linear dimension of the antenna aperture and λ the free-space wavelength. When assuming a circular aperture with uniform illumination both in amplitude and phase, the power density on the axis of the antenna in the near field region varies as a function of distance with maxima equal to four times the power density at the aperture. These maxima occur out to the transition to the far field. Beyond this distance, the power density falls off and approaches the inverse square relation as the distance increases.

Using D as the widest dimension of the horn, the far field was found to be beyond:

$$\frac{2(D)^2}{\lambda} = \frac{2(32.067)^2}{12.24} \tag{7}$$

$$= 167.88 \text{ cm.}$$

It was decided that the probes of the commercial instrument should be calibrated at mid-scale reading at the power density levels being used in this research. Therefore, 10 mW/cm^2 and 100 mW/cm^2 were chosen.

The distance, R, at which a power density of 10 mW/cm^2 would be obtained was calculated.

$$R = \frac{P_t G}{4\pi P_D} = \frac{(250 \times 10^3)(45.01)}{4\pi (10)} \qquad (8)$$

$$R = 299.32 \text{ cm.}$$

The distance to observe 100 mW/cm^2 was

$$R = \frac{(250 \times 10^3)(45.01)}{4\pi (100)}$$

$$R = 94.65 \text{ cm.}$$

Movable absorbing material was placed around the calibration range to minimize any scattered and reflected waves. Using the probe with mid-scale readings of 10 mW/cm^2 and 100 mW/cm^2, a $\frac{1}{R^2}$ plot was made and showed observed levels that agreed with calculated values to within ±1 dB. The middle range probe (mid-scale readings of 1.0 mW/cm^2 and 10 mW/cm^2) was evaluated at 10 mW/cm^2 and was also found to be within ±1 dB. Slight variations in probe readings may result from scattered radiation, probe orientation, "zeroing" of the scale settings, etc.

Output Frequency

The magnetron output frequency was determined by attaching a frequency meter, a thermistor and power meter to the attenuator on the side arm of the directional coupler. The center frequency was found to be 2423 MHz and remained constant with input currents over the range of 0.1 to 0.5 Amperes.

A spectrum analyzer was used to determine the bandwidth of the output around the center frequency. The bandwidth also appeared to be independent of input currents between 0.1 and 0.5 Amperes and was determined to be 100 kHz at the half-power points. Figures 13 and 14 show the spectrum as observed. Figure 13 shows the spectrum with a oscilloscope horizontal scale of 300 kHz per cm and a vertical scale of 10 dB per cm. Figure 14 shows the same spectrum with a horizontal scale of 1 MHz per cm and the same vertical scale of 10 dB per cm.

From the detailed information presented, it can be seen that it is entirely feasible and practical to construct an accurately calibrated, compact and relatively inexpensive microwave system to irradiate small biological specimens. Total cost for the system is less than $10,000 and was effectively designed so that it was possible to place the complete system in a room of less than 11.0 m^2.

It is seen that the system provides a beam within 1 dB uniformity over a circular area with a diameter of about ½ wavelength ($\sim$ 6 cm) and a 3 dB uniformity over about one wavelength (12.24 cm). It is possible to provide continuous output at any selected power density up to and exceeding 1.0 W/cm^2.

With an input power of 900 Watts, and 250 Watts directed to the

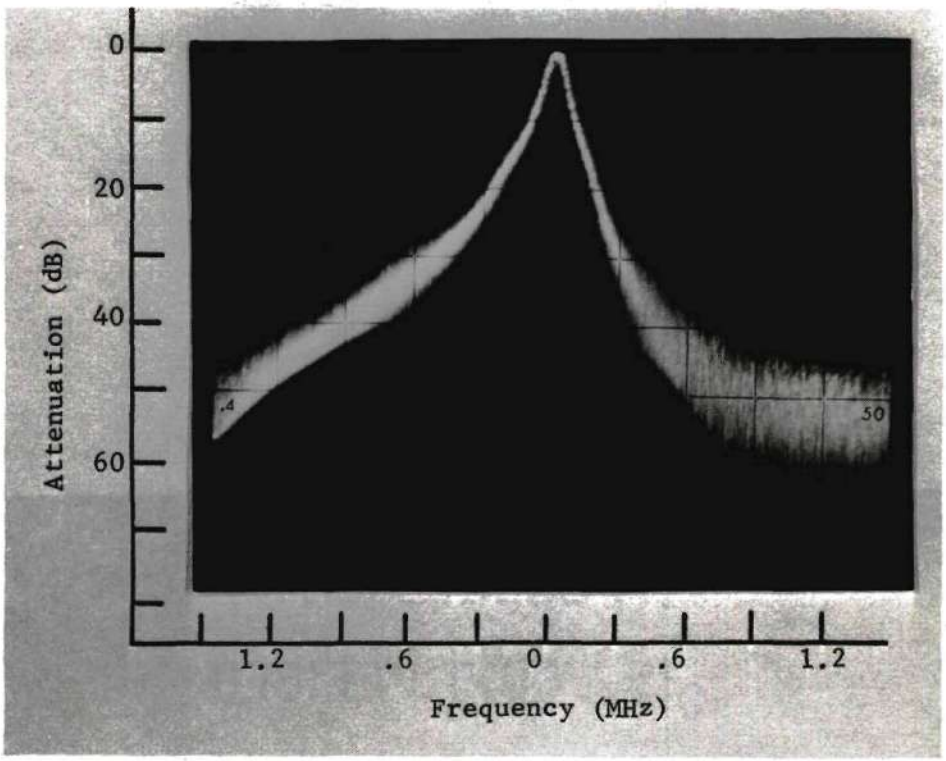

Figure 13. Spectrum Bandwidth

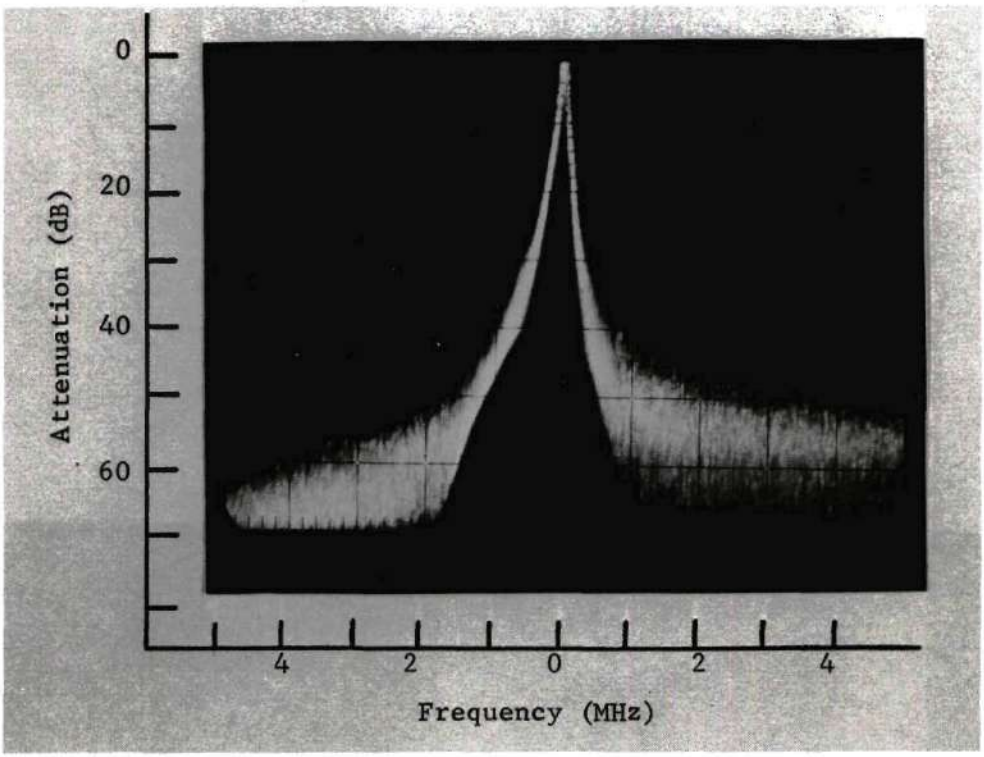

Figure 14. Spectrum Bandwidth

antenna, it is seen that there is an efficiency of about 28%. The coupling efficiency from the antenna is about 35% when considering the half power area of 117.67 cm^2 and the approximate power density of 0.75 W/cm^2.

CHAPTER IV

BIOLOGICAL CONSIDERATIONS AND EXPERIMENTAL PROCEDURE

Platelets

The human platelet is a round or oval cell about 2 to 4 microns in diameter. The term cell should probably not be applied, however, since the platelet is a nonnucleated cytoplasmic fragment derived from the megakaryocyte.[73,74] There are normally between 200,000 and 400,000 platelets per cubic millimeter of human whole blood. The disintegration of one mature megakaryocyte results in the production of 3,000 to 4,000 platelets. As with other hematopoietic cells, the platelets then pass through the walls of the bone marrow to enter the circulatory system.[74-76] It is generally accepted that platelets have a maximum *in vivo* survival time of 8 to 10 days and that their size decreases with age. Upon removal from the circulatory system, however, platelets rapidly lose their viability so that handling or storage should not exceed a few hours or at most about one day. Circulating platelets possess a high negative surface charge due in part to sialic acid residues of the glycoprotein component of the platelet membrane.

The Role of Platelets in Coagulation

The role of platelets in the blood coagulation process was not demonstrated until 1882; and, as recently as 1920, even the existence of platelets as distinct entities was disputed. The ability of platelets to stick together and to damaged blood vessel walls is the

basis for their hemostatic function. Masses of platelets also contribute to the abnormal and sometimes lethal clots, or thrombi, within coronary arteries and other blood vessels. Platelets will tend to stick to any glass material as well, and it is for this reason that all such surfaces used in the laboratory analysis procedures must be siliconized.

Within seconds after a cut occurs in a vessel, the platelets begin to adhere to the surface. Within a minute or so, more platelets stick to the first ones and enough are collected to form a whitish plug which rapidly solidifies and bleeding ceases. The formation of this plug depends in part on thrombin, an enzyme which is an important key in blood clotting. Thrombin converts the soluble plasma protein fibrinogen into insoluble fibrin, which forms a solid meshwork in a clot. Thrombin is not present in circulating blood, but is generated from an inactive precurser, prothrombin, when it is needed for hemostasis.[74] Individuals suffering from hemophilia bleed excessively because their blood lacks one of the plasma proteins necessary to convert prothrombin into thrombin. This deficiency prevents the rapid evolution of thrombin necessary for forming the platelet plugs.

Research by Lamb *et al.*,[64] has shown that there is a definite electrical effect on the coagulation time of whole blood. They found that both *in vitro* coagulation of dog whole blood and *in vivo* thrombosis of blood vessels are voltage dependent, and that the critical potential difference below which such action does not occur is about 2 Volts. Richardson[65] has performed studies on coagulation times in dog blood using 2450 MHz radiation and has shown that the times may be

either increased or decreased depending on exposure time, and perhaps many other not yet understood variables.

Experimental Procedure

As will be seen, the methodology and procedures used in this research depend on techniques involving a wide variety of disciplines. For this reason, it is the purpose of this section to outline in complete detail the specific procedures used in order to allow an individual to duplicate the study no matter what his discipline.

Sample Preparation

Human blood must be collected just prior to each run and is collected by drawing 4.0 ml of blood into a siliconized vacutainer tube containing 1.0 ml of 3.8 percent sodium citrate. The sodium citrate is an anti-coagulant which prevents coagulation by absorbing calcium ions. In order to avoid tissue thromboplastin, the first few drops of blood are allowed to drop from the needle into an adapter sleeve before the vacutainer tube is inserted into the sleeve. Filling of the tube takes approximately five seconds. Sufficient tubes are collected to allow an ample supply for each experimental run. (Six to eight tubes were typically collected.) The tubes are then gently inverted twice to allow for careful mixing and allowed to sit for ten minutes.

To prepare the platelet-rich plasma, the stopper of the vacutainer tube is removed and the blood centrifuged for five or ten minutes at 800 revolutions per minute. The platelet-rich plasma is removed using a siliconized syringe and placed in a siliconized beaker where it

is gently agitated to provide uniform mixing. The plasma is then placed in the appropriately prepared vials to be used for the irradiation of the samples.

The vials used in this research are glass and rectangular in shape, approximately 2.0 cm on each side and 5.9 cm in height. The top is covered with a plastic screw cap. The wall thickness is about 0.10 cm. Each vial is siliconized and filled with 2.0 ml of platelet-rich plasma.

Irradiation Procedure

In order to turn on the microwave source, the switch on the junction box used to supply power to the power supply is placed in the "on" position.

Flip the "power on" switch up in order to adequately heat the elements in the magnetron tube and in the power supply. The orange indicator light indicates that this step has been completed. After about a three minute delay the second orange "ready" light comes on to indicate that adequate warm-up time has been allowed.

Prior to activating the high voltage, check to insure that the doors to the power supply are closed and that the variac is in a fully counter-clockwise position.

Remove the wooden support from in front of the antenna which is used to brace the cantilevered antenna feed. Check to insure that the shielding is in place and that all material other than the sample support structure is removed from the microwave field. See that the feed, antenna, and sample support structure are in the proper location.

Check to insure that the sliding short circuit is placed so that all or nearly all of the generated power will be diverted into the high-power load.

Push high voltage button on and be sure that the red light is lit.

Perform a radiation safety survey of the entire microwave exposure system to insure that no hazardous levels are leaking from the system and check the entire working environment for any stray radiation. This survey is performed with a portable microwave survey meter. Check to see that the batteries are charged, that the proper probe is being used, and that the instrument is set to detect the 2450 MHz frequency.

Place the calibrated receiving antenna (in this case, the portable detector) on the sample support structure at the focal point of the microwave beam.

Turn the variac in a clockwise direction until the magnetron input current stabilizes at 0.3 Amperes and the input voltage is approximately 3.0 kilovolts.

Slowly adjust the tandem short circuit until the approximate power density desired is obtained. Observe the receiving antenna indicator and fine-tune the tandem short circuit. Wait about five minutes for the system to stabilize and again fine-tune the output power density.

Turn down the variac, remove the receiving antenna, place the samples to be irradiated on the sample support structure, being careful to have the front face of the sample container parallel to the aperture of the antenna, and re-set the variac to the 0.3 Ampere input current.

Perform an additional radiation survey to see that no stray radiation results from the increased power density levels.

Place appropriate warnings around the system so that no personnel in the area can inadvertently walk into the hazardous radiation areas.

If the temperature rise is being monitored from a separate sample vial located at the focal point (using the special mercury thermometer calibrated for temperatures of about 20°C to 40°C), see that the same temperature is maintained in the control sample. The control sample is placed in a temperature controlled water bath and the temperature carefully controlled with another previously calibrated thermometer. This control sample is placed in an area away from any microwave fields.

At the end of the irradiation period, turn down the variac, push in the "high voltage off" button (the red light goes out), wait about three to five minutes for the fans to cool down the magnetron tube, and flip down the "power off" switch.

The switch on the junction box is placed in the off position.

As a safety precaution, readjust the tandem short circuit so that all power will again be diverted into the high power load.

Replace the wooden support used to brace the cantilevered antenna feed.

Platelet Counting by Phase Microscopy

To prepare for platelet counting, the platelet-rich plasma is gently mixed and drawn into disposable blood diluting pipettes. These pipettes contain a given amount of ammonium oxalate to produce a

dilution ratio of 1:100.

Place a clean cover glass on the counting chamber. Gently agitate the pipette for one minute. Discard several drops from the pipette and place a drop of the plasma on the surface of the counting chamber at the edge of the cover glass. The diluted plasma is drawn rapidly by capillary action into the space between the cover glass and the ruled area of the chamber.

The counting chamber is placed in a closed Petri dish containing a damp filter paper and left for 20 minutes to allow the platelets to settle.

Place the chamber on the phase microscope stage. Find the ruled area and use a magnification of 400 to count the number of platelets in one square millimeter. The number of platelets per cubic millimeter is determined by counting the platelets in one square millimeter on both sides of the chamber, dividing by two, and multiplying the number by 1,000.

Coagulation Determination

Medical laboratories use various methods for determining the clotting characteristics of blood. The thrombelastograph is probably the most reliable and most sophisticated method yet developed, and is the method chosen for this research. This technique utilizes the optical registration of clot formation on the basis of the developing elastic properties of the plasma clot. It permits a simultaneous and continuous visual, as well as photographic, observation of up to three plasma specimens during all phases of coagulation, at a controlled temperature of 37°C and with complete exclusion of air.

A small stainless steel cylinder is suspended into a small slowly oscillating cup (period equal to 9.0 seconds) into which the plasma is placed. In the unclotted state, the suspended cylinder remains essentially stationary in the plasma as the cup oscillates. As soon as the surface of the cylinder becomes connected with the wall of the cup by a sufficient number of fibrin threads having elastic properties, the cylinder begins to turn with the cup. The cylinder in each sample is suspended by a thin wire. On this torsion wire is mounted a small mirror which reflects a small beam of light. The movement of the cylinder, torsion wire, mirror and light beam are directly visible and are also recorded on a moving film (moving at two mm per minute). Before the cylinder begins to move, the light beam is stationary and therefore produces a single line on the film. The time elapsing before the line begins to split (start of cylinder movement) is called the reaction time (r value). This time is considered to represent the coagulation time. The rate at which the elasticity of the clot increases is measured as the time required to reach a spread of 20 mm between the two lines on the film (k value). The maximum distance reached between the two lines is called the clot strength (ma value). This resulting configuration is called a thrombelastogram and is shown in Figure 15.

The clotting time is highly dependent on the function of the coagulation mechanism, whereas the shape of the thrombelastogram is determined by the quantity and function of the fibrinogen and platelets.[77]

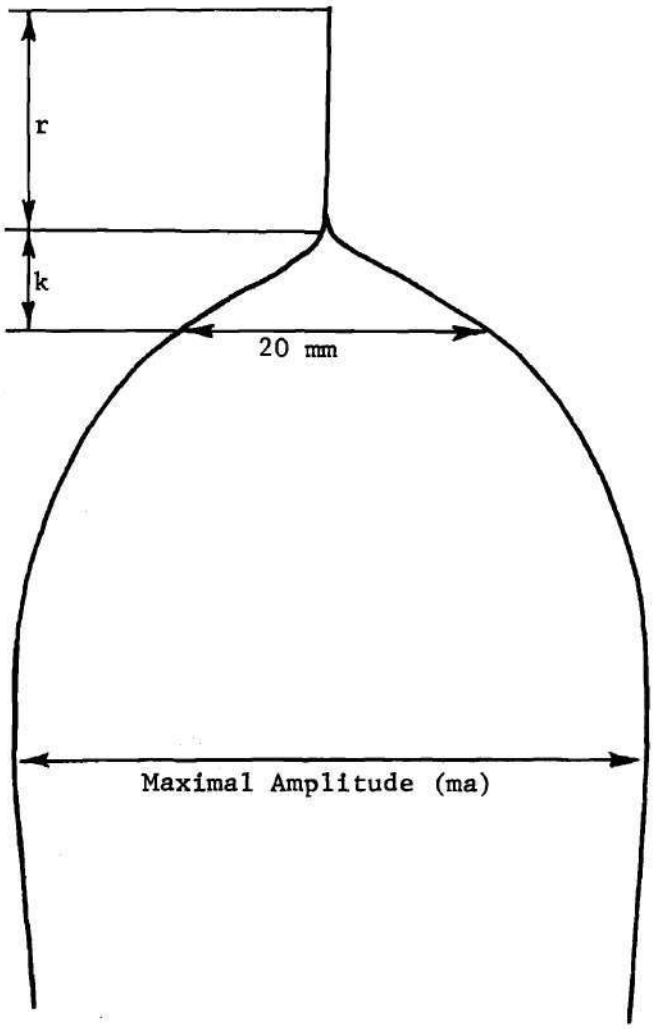

Figure 15. Diagram of a Normal Thrombelastogram

Carefully measure a 0.25 ml sample of the platelet-rich plasma and place it in the appropriate cup which has been prewarmed for five minutes at 37°C.

After a one minute wait, add 1/10 ml of 1.29% calcium chloride and immediately lower the cylinder into the cup. Add sufficient mineral oil to completely cover the sample.

Visually observe the movement of the light beam and allow sufficient time for the thrombelastogram to be properly recorded.

CHAPTER V

DIELECTRIC AND ABSORBED POWER ANALYSIS

A review of the literature on studies of biological effects from microwave radiation indicates that serious questions can be raised on the reported powers and power densities used in various research. Typically, the reports fail to describe the techniques employed in determining the exposure levels used, and there may be little or no relationship to the actual power absorbed within the biological specimen.

In an attempt to present more meaningful information to relate microwave exposure to the biological effects, considerable effort has been made in this study to develop a uniform field for the irradiation in which the incident power densities can be precisely determined.

It was felt desirable, additionally, to determine the microwave power absorbed within the plasma. This was done since, at the present time, there are no acceptable or standardized procedures for microwave dosimetry techniques. Proper and effective instrumentation is needed and must be developed. However, it is possible to go beyond measurement of only incident power densities when evaluating microwave effects to biological systems, and to determine the actual power absorbed.

The power absorbed within the plasma is a function of the incident power and is related to the interface characteristics of the sample and sample holder. The Fresnel type reflections at the interfaces and the molecular absorption can be evaluated and accounted for

by knowing the dielectric constant, loss tangent and physical dimensions of the sample and sample holder. In order to perform this, it was necessary to construct a system which would allow for the accurate measurement of parameters needed to calculate the dielectric constant and loss tangent of the plasma.

Dielectric Constant Determination

The technique used has been described by Altschuler[78] and a brief review of the theory as presented is appropriate. The procedure is a two-point method of measuring the dielectric constant which involves the solution of a transcendental equation.

The theory underlying this method is based on consideration of Figure 16. Figure 16(a) shows an empty short-circuited waveguide with a slotted line probe located at a voltage minimum D_R. Figure 16(b) shows the same waveguide, now containing a sample of length ℓ_ϵ with the probe located at a new voltage minimum D. The sample must be adjacent to the short circuit. Looking from $T_{\epsilon 1}$ towards the right and left, the following impedance equation can be written:

$$Z_o \tan k\ell = - Z_\epsilon \tan k_\epsilon \ell_\epsilon \qquad (9)$$

where:

Z_o = characteristic impedance

k = propagation wave number

ℓ = sample to voltage minimum distance

Z_ϵ = sample impedance

k_ϵ = sample wave number

ℓ_ϵ = sample length

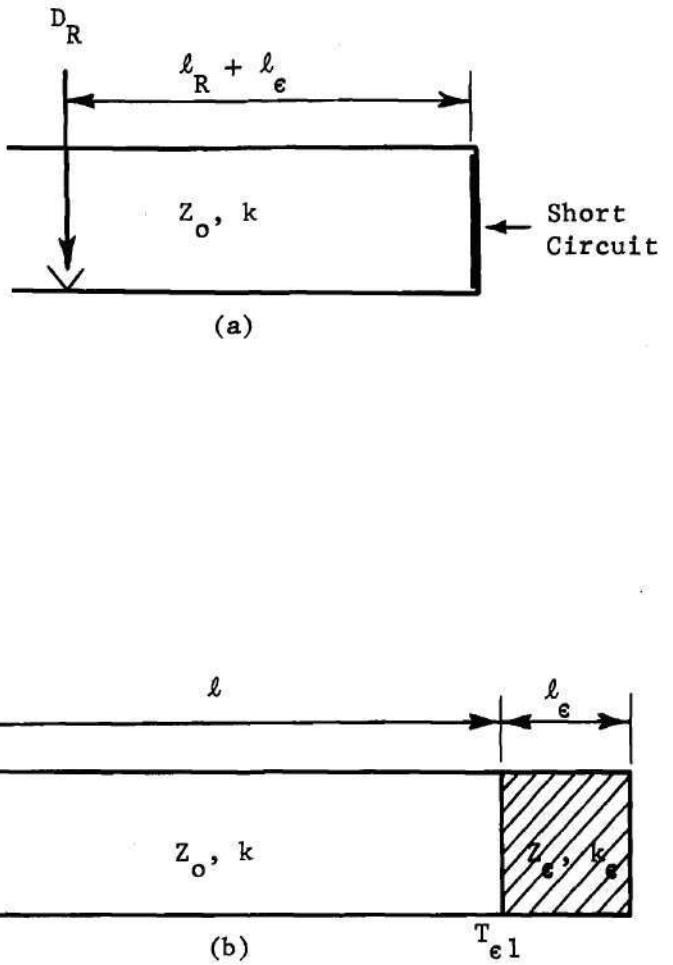

Figure 16. Dielectric Constant Measurement with Short-Circuited Waveguide[78]

Likewise, in Figure 16(a), looking toward the right, one has

$$Z_o \tan k(\ell_R + \ell_\epsilon) = 0 \quad . \tag{10}$$

Now, consider

$$\tan k(D_R - D + \ell_\epsilon) = \tan k\left[(\ell_R + \ell_\epsilon) - (\ell + \ell_\epsilon) + \ell_\epsilon\right]$$

$$= \tan k\left[(\ell_R + \ell_\epsilon) - \ell\right] \quad .$$

Upon expanding the tangent and making use of Equation (10), substitution into Equation (9) yields

$$Z_o \tan k(D_R - D + \ell_\epsilon) = Z_\epsilon \tan k_\epsilon \ell_\epsilon \quad . \tag{11}$$

Since $Z_o/Z_\epsilon = k_\epsilon/k$, one can rewrite Equation (11) in the form,

$$\frac{\tan k(D_R - D - \ell_\epsilon)}{k\ell_\epsilon} = \frac{\tan k_\epsilon \ell_\epsilon}{k_\epsilon \ell_\epsilon} \tag{12}$$

It is now noted that all the quantities associated with the left-hand member are measurable, while the right-hand member is of the form $\tan Z/Z$, so that once the measurement has been performed, the complex number, $Z = k_\epsilon \ell_\epsilon$, can be found by the solution of the transcendental equation and from it, k_ϵ. ϵ_r is then found from

$$k_\epsilon = \frac{2\pi}{\lambda} \sqrt{\epsilon_r \mu_r - \left(\frac{\lambda}{\lambda_c}\right)^2} \tag{13}$$

where:

λ = free space wavelength

ϵ_r = dielectric constant

μ_r = relative permeability

λ_c = cut-off wavelength

In view of the periodic nature of the tangent function, there exists an infinity of solutions for ϵ_r. It is consequently either necessary to know ϵ_r approximately in order to pick the right solution, or to perform a second identical experiment with a sample of different length ℓ_ϵ. The proper solution in the latter case is the one common to the two sets of solutions. This is an "intersection point," as demonstrated in Figure 17 for a particular case.

For plasma and other lossy dielectrics, equation (12) is recast to achieve a more practical form as will be seen.

The equipment used in this measurement procedure includes a signal generator set at 2450 MHz and modulated with 1000 MHz square waves, coax-to-waveguide adapter, variable flap attenuator, slotted line with probe connected to a VSWR meter, 90° E-plane bend (allowing the short circuit to be horizontal and thus allowing the liquid plasma to be level and in complete contact with the short) and finally the short circuit.

The plasma samples are prepared in a similar manner to that previously described in Chapter IV. The short circuit was siliconized and its dimensions were determined to be 3.39 cm by 7.22 cm, giving an effective area of 24.48 cm^2. The plasma was measured and placed into the short circuit with a siliconized 1.0 and 10 ml pipette. The

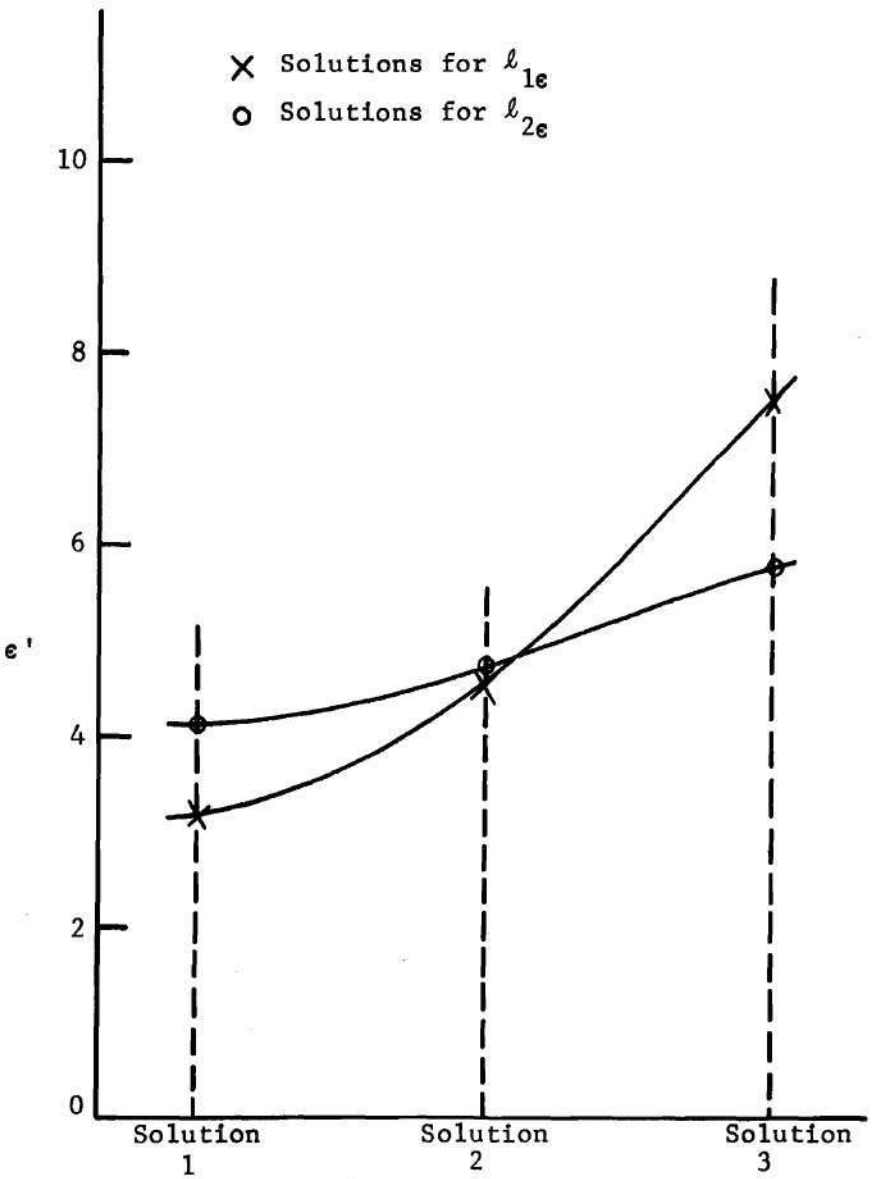

Figure 17. Solution for ε' Obtained from the Measurement of Two Different Length Samples of the Same Material[78]

following volumes were used to obtain the desired heights:

Height (cm)	Volume (ml)
0.3	7.34
0.4	9.79
0.5	12.24
0.6	14.69
0.7	17.14
0.8	19.59
0.9	22.04

Experimental Procedure

Connect the equipment in the order as previously mentioned. With no sample dielectric in the shorted line, find D_R, the position of the minimum in the slotted line with respect to any arbitrary chosen reference plane. (A micrometer gauge is helpful in making these measurements.)

Adjust the VSWR meter to obtain a reading of 3.0 on the dB meter scale. Move the slotted line probe to each side of the voltage minimum and obtain a full-scale reading (0 dB) on the scale. Record the probe positions at these two equal readings.

Measure the guide wavelength, λ_g, by measuring the distance between alternate minima in the slotted line.

Remove the short circuit and pipette the desired amount of plasma into the waveguide so that the short circuit acts as the base of a container for the plasma.

Measure D, the position of the new minimum in the slotted line with respect to the reference plane. This new minimum must be measured in a direction toward the generator, with respect to D_R, and in a positive direction.

Observe the VSWR from the meter scale and also determine the 3 dB points as before.

Repeat the procedure for other heights of blood plasma.

Dielectric Constant Calculations

For "lossy" material such as water or blood plasma, the calculations are as follows:

(1) Determine the standing-wave ratio:

$$r = \frac{\lambda_g}{\pi(X_o)} \tag{14}$$

where λ_g = guide wavelength

X_o = distance between 3 dB points.

(2) Determine the propagation wave number

$$k = \frac{2\pi}{\lambda_g} \tag{15}$$

(3) Compute $\Phi = 2k(D - D_R - \ell_\epsilon)$ (16)

(4) Compute $|\Gamma| = \frac{r - 1}{r + 1}$ (17)

(5) Determine the complex number

$C\angle\Psi$ from:

$$C\angle-\Psi = \frac{1}{jk\ell_\epsilon} \frac{1 - |\Gamma| e^{j\Phi}}{1 + |\Gamma| e^{j\Phi}} \tag{18}$$

(6) Solve the complex transcendental equation below for T and τ:

$$C\angle-\Psi = \frac{\tanh (T\angle\tau)}{T\angle\tau} \tag{19}$$

An extensive plot of these solutions is available in the literature.[79]

(7) Compute the admittance determinant Y_ϵ from:

$$Y_\epsilon = \left(\frac{T}{k\,\ell_\epsilon}\right) \angle 2(\tau - 90^\circ) \tag{20}$$

(8) Compute the dielectric constant ϵ_r from:

$$\epsilon_r = \frac{Y_\epsilon + \left[\frac{\lambda_g}{\lambda_c}\right]^2}{1 + \left[\frac{\lambda_g}{\lambda_c}\right]^2} \tag{21}$$

where λ_c = twice the wide dimension of the waveguide.

In order to check the reliability of the measurement system which was fabricated and the accuracy of the calculations, the technique was first tested using water at 23°C and comparing the results with those values reported by vonHippel.[79]

The data shown in Table I was observed. From this, the following results were obtained:

height(cm)	ϵ_r
0.3	77.4
0.4	71.6
0.8	74.0
0.9	76.7

vonHippel reports ϵ_r values for water at 25°C of 77.5 at 300 MHz and 76.7 at 3,000 MHz.

The procedure was then repeated using the blood plasma at 23°C as the dielectric sample. The data as collected is shown in Table 2.

The following is a sample calculation using the data obtained to determine the dielectric constant for blood plasma:

Table 1. Observations for Determining the Dielectric Constant of Water

Sample Height (cm)	Water Sample Present*	
	Voltage Minimum (cm)	Distance Between 3 dB Points (cm)
0.3	10.96	0.55
0.4	1.21	1.60
0.8	0.71	0.13
0.9	0.67	0.25

*With no dielectric sample present, the voltage minimum was arbitrarily set at 0.0 cm and the distance between the 3 dB points was 0.04 cm.

Table 2. Observations for Determining the Dielectric Constant of Blood Plasma

Sample Height (cm)	Blood Plasma Sample Present*	
	Voltage Minimum (cm)	Distance Between 3 dB Points (cm)
0.4	15.37	2.09
0.5	15.64	0.66
0.6	15.61	0.33
0.7	15.62	0.23

*With no dielectric sample present, the voltage minimum was at 14.87 cm and the distance between the 3 dB points was 0.03 cm.

Given: $\lambda_g = 22.98$ cm

$\ell_\varepsilon = 0.4$ cm

$D_R = 14.87$ cm

$D = 15.37$ cm

$X_o = 2.09$ cm

Therefore:

$$r = \frac{22.98}{\pi(2.09)}$$

$$= 3.4999$$

$$k = \frac{2\pi}{22.98}$$

$$= 0.2734$$

$$\Phi = 2(0.2734)(15.37 - 14.87 - 0.4)$$

$$= 0.0547$$

$$|\Gamma| = \frac{2.4999}{4.4999}$$

$$= 0.5555$$

Therefore:

$$C\angle -\Psi = \frac{1}{j(0.2734)(0.4)} \frac{1 - 0.5555\ e^{j0.0547}}{1 + 0.5555\ e^{j0.0547}}$$

Since:

$$e^{j0.0547} = \cos 0.0547 + j \sin 0.0547$$

$$= 0.9985 + j0.0547$$

$$C\angle -\Psi = -j9.1441 \frac{1 - [0.5555(0.9985 + j0.0547)]}{1 + [0.5555(0.9985 + j0.0547)]}$$

$$C\angle -\Psi = -j9.1441 \frac{0.4453 - j0.0304}{1.5547 + j0.0304}$$

$$C\angle -\Psi = \frac{-0.2780 - j4.0719}{1.5547 + j0.0304}$$

When converted to polar coordinates:

$$C\angle -\Psi = \frac{4.0814\angle -93.9057^\circ}{1.5550\angle +1.1202^\circ}$$

and

$$C\angle -\Psi = 2.6247\ \angle -95.0259^\circ$$

Therefore:

$$C = 2.6247$$

$$1/C = 0.3810$$

$$\Psi = -95.0259^\circ$$

From the graphical plots:

$$T = 1.63$$

$$\tau = 82^\circ$$

and

$$Y_\epsilon = \left(\frac{1.63}{(0.2734)(0.4)}\right)^2 \angle 2(82^\circ - 90^\circ)$$

$$= 222.1561\ \angle -16.0^\circ$$

and

$$\epsilon_r = \frac{222.1561 + \left[\frac{22.98}{14.44}\right]^2}{1 + \left[\frac{22.98}{14.44}\right]^2}$$

$$= 63.6043$$

Similar calculations were performed at other plasma sample heights and the following dielectric constants were obtained:

Height (cm)	ϵ_r
0.4	63.6
0.5	64.4
0.6	64.9
0.7	63.5

Loss Tangent Calculations

The relative dielectric constant can be written in the form

$$\epsilon_r = \epsilon' - j\epsilon'' \tag{22}$$

where ϵ' is associated with the ability of the dielectric material to store electric energy and ϵ'' with the dielectric losses that occur in the material.[78]

It is also useful to write the relative dielectric constant as

$$\epsilon_r = \epsilon'(1 - j \tan \delta) \tag{23}$$

Therefore:

$$\tan \delta = \frac{\epsilon''}{\epsilon'} \quad . \tag{24}$$

The quantity tan δ is usually referred to as the loss tangent. It is proportional to the ratio of the power lost in heat (by means of dielectric loss) to the energy stored per cycle and therefore is a good measure of how "lossy" a dielectric material is.

Y_ϵ as previously defined is a complex quantity and may be written in rectangular form as:

$$Y_\epsilon = G_\epsilon + j K_\epsilon \tag{25}$$

When the measurement is performed in rectangular waveguide, equation (21) becomes:

$$\varepsilon' = \frac{G_\varepsilon + \left[\frac{\lambda_g}{\lambda_c}\right]^2}{1 + \left[\frac{\lambda_g}{\lambda_c}\right]^2} \tag{26}$$

and

$$\varepsilon'' = - \frac{K_\varepsilon}{1 + \left[\frac{\lambda_g}{\lambda_c}\right]^2} \tag{27}$$

A continuation of the sample calculation just given produces the following:

$$Y_\varepsilon = 222.1561 \angle -16^\circ$$

When changed to rectangular form:

$$Y_\varepsilon = 213.5501 - j61.2345 \quad .$$

Therefore:

$$G_\varepsilon = 213.5501$$

and

$$K_\varepsilon = - 61.2345 \quad .$$

From equation (26):

$$\varepsilon' = \frac{213.5501 + \left[\frac{22.98}{14.44}\right]^2}{1 + \left[\frac{22.98}{14.44}\right]^2}$$

$$= 61.1682$$

and from equation (27):

$$\epsilon'' = \frac{61.2345}{3.5326}$$

$$= 17.3341 \quad .$$

Therefore, from equation (24):

$$\tan \delta = \frac{17.3341}{61.1682}$$

$$= 0.2834$$

Repeating these calculations for each of the sample heights produces the following loss tangent values (shown with the corresponding dielectric constants):

Height(cm)	ϵ_r	tan δ
0.4	63.6	0.2834
0.5	64.4	0.3249
0.6	64.9	0.3211
0.7	63.5	0.3021

Absorbed Power

An investigation of the ratio of the power absorbed within the plasma sample to that of the incident power density as determined with the receiving antenna gives a more meaningful indication of the true microwave effects to the plasma or any other biological specimens. Such an investigation of this multilayer system consisting of an air-glass interface, a glass-plasma interface, a plasma-glass interface, and finally a glass-air interface has been made with the use of a digital computer program for calculating the complex transmission coefficient and reflection coefficient of plane, "lossy" multilayer systems.

The computer program is based on work performed by Richmond[80] and Breeden[81] using matrix multiplication to study multilayer systems for normal incidence where the electric field intensity vector is perpendicular to the plane of incidence (perpendicular polarization). The program is written in Fortran IV language for running on the UNIVAC 1108 system at Georgia Tech. The computer program is given in Appendix A.

The following information was used in the analysis.

	Relative Dielectric Constant	Loss Tangent	Layer Thickness (Inches)
Layer 1 (glass)	4.2	0.005	0.105
Layer 2 (plasma)	64.0	0.300	0.590
Layer 3 (glass)	4.2	0.005	0.105

It can be seen from Appendix A that the percent of incident power reflected equals 67.3, the percent of incident power transmitted through the entire system is 8.5, and the percent of incident power absorbed by the complete structure equals 24.2. Since the glass has a low loss tangent, it has been considered as a lossless medium and assumed that all or nearly all of the abosrbed power is in the "lossy" plasma.

The 2.0 ml of plasma placed in the sample vials as previously described presents an incident surface area of 1.142 cm^2. Therefore, it can be seen that for each mW/cm^2 of power density incident on the sample, 0.276 mW of power is absorbed in the sample.

CHAPTER VI

EXPERIMENTAL RESULTS

Blood was drawn from nine individuals over a period of about four months. Thirty-seven runs were made with a total of 162 samples being used in the irradiations. The amount of blood drawn per run averaged about 25 ml and in all cases was drawn from individuals within one hour of the start of the irradiation.

For each run, at least one control sample was used and kept at the same temperature as the irradiated samples. The thermometers used to register any temperature changes were intercalibrated to $\pm 1^{\circ}C$ over a temperature range of $0^{\circ}C$ to $100^{\circ}C$ both with and without the effects of a microwave field.

In those samples where a significant temperature rise was observed, it was noted that the rise above the ambient room temperature (about $23^{\circ}C$) occurred within 30 to 45 minutes followed by a "leveling off" and a resulting equilibrium temperature.

While the reported data is always related to a relative value of 1.0 assigned to the platelet count of the control for each run, it is worth noting that the number of platelets per mm^3 averaged about 400,000 immediately after being drawn and showed a counting accuracy of about $\pm$ 7%. This varied from a minimum of 94,000 to a maximum of 475,000. Average coagulation time and clot strength were determined from the thrombelastograms. A typical thrombelastogram for three samples is shown in Figure 18. Using the description as shown in

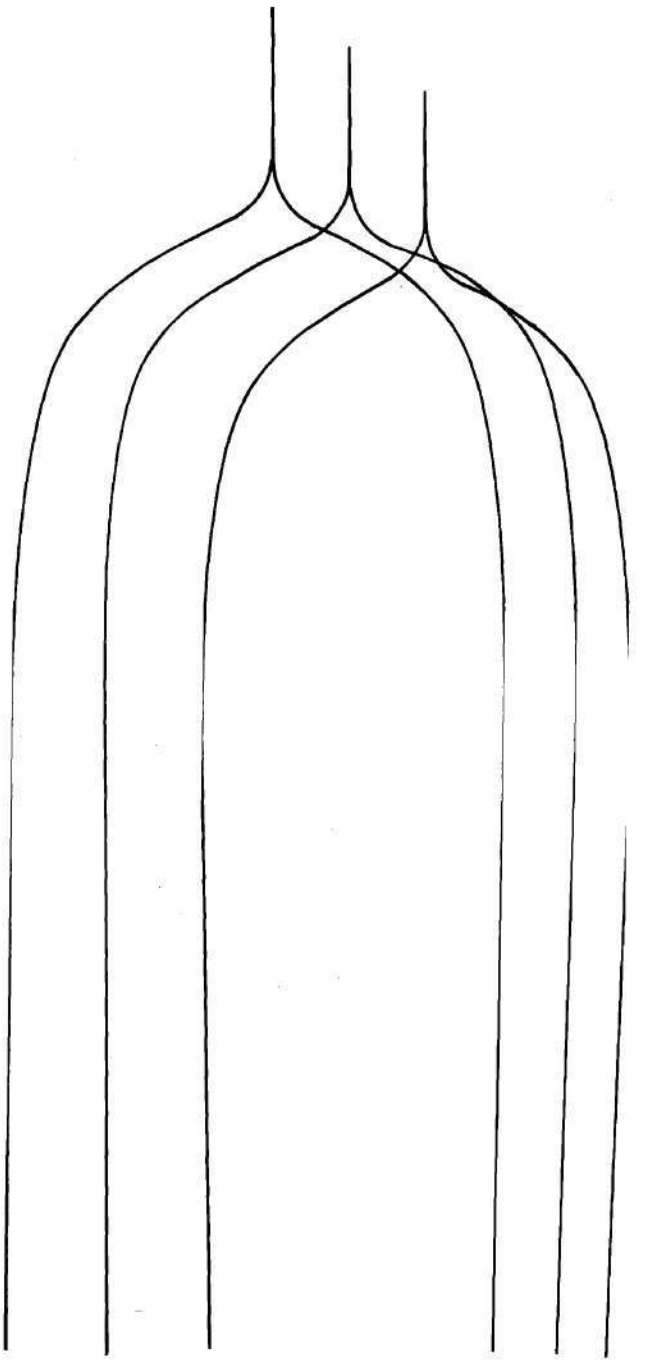

Figure 18. Typical Thrombelastogram of Three Samples

Figure 15, typical coagulation times of 10.0 minutes (20.0 mm on the thrombelastogram) and clot strengths of 60 mm were observed.

The data in Table 3 and illustrated in Figure 19 show that there is no significant effect on the platelet count for incident power densities between 10 mW/cm^2 and 280 mW/cm^2. This corresponds to absorbed power levels of 2.7 mW to 77 mW. The exposure time was held constant at 5.5 hours and in all cases the plasma temperature was maintained below 37°C, the normal body temperature.

A sample of the calculations and definitions used to statistically analyze the data is shown in Appendix B. The results of the analysis show the following:

$$\bar{Y} = 1.0019$$

$$Y_{rms} = 1.0081$$

$$\sigma y = 0.1118$$

$$r = 0.2102.$$

The estimating equation is:

$$Y = 0.000267X + 0.97786 \quad .$$

Assuming a t-distribution of the data:

$$\bar{X} = 1.00192 \pm 0.04595$$

for 95% confidence limits.

Table 4 and Figure 20 present data showing that no significant effect is apparent on coagulation time as a function of power density between 10 mW/cm^2 and 280 mW/cm^2, or (for the experimental conditions in this research), absorbed power between 2.7 mW and 77 mW. As before,

Table 3. Incident Power Density and Relative Platelet Count for 5.5 Hour Exposure Times and Temperatures Remaining Below 37°C

Power Density Incident on Sample Container (mW/cm^2)	Relative Platelet Count
10	1.11
10	0.97
10	1.05
10	0.78
10	1.16
25	1.09
25	1.08
25	0.90
25	0.92
50	0.96
50	0.97
50	0.88
60	0.99
60	0.95
100	1.24
100	1.18
100	0.99
100	0.84
100	0.88
100	0.99
100	0.92
100	0.94
280	1.04
280	0.95
280	1.18
280	1.09

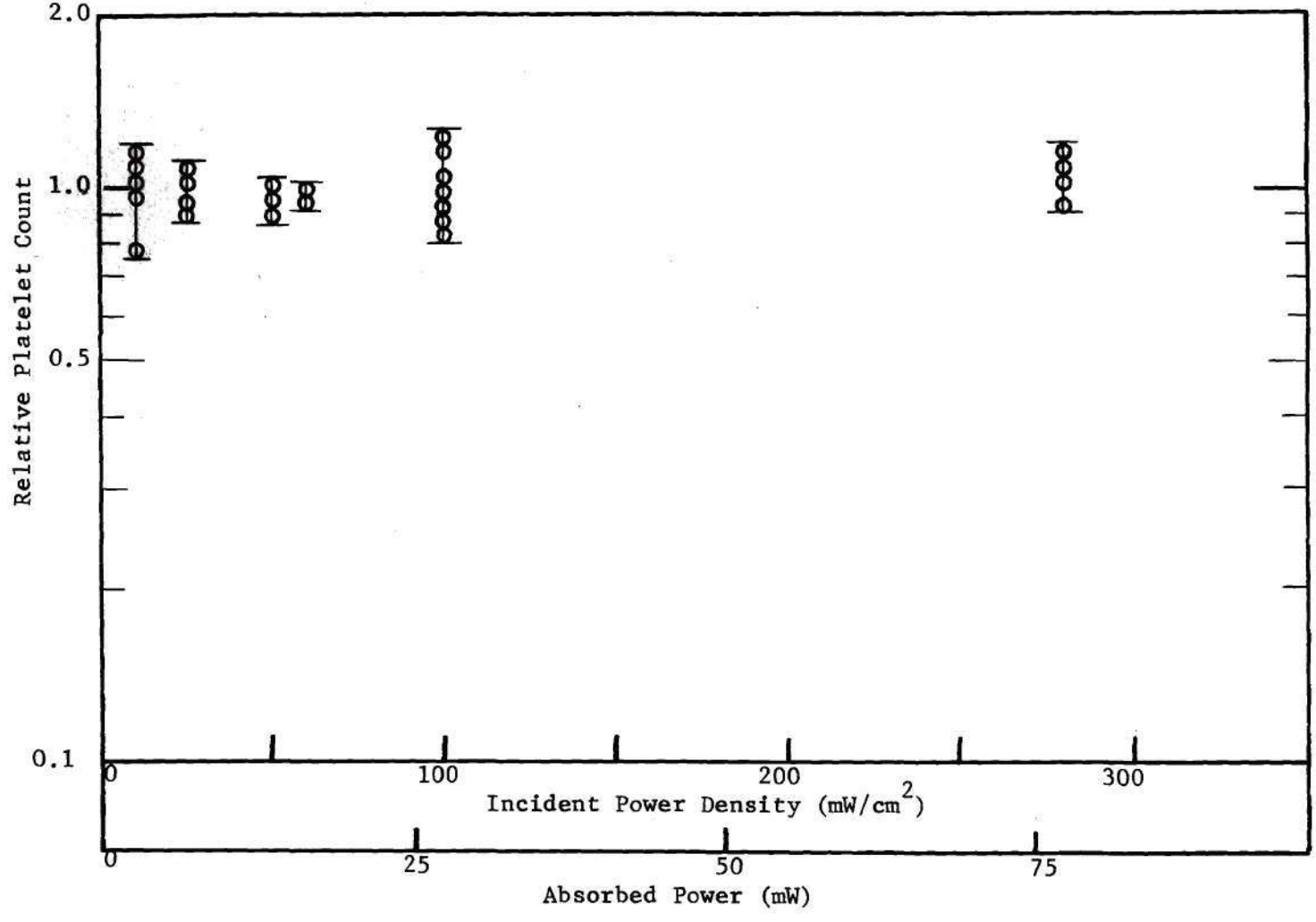

Figure 19. Relative Platelet Count vs. Incident Power Density and Absorbed Power for 5.5 Hour Exposures and Temperatures Remaining Below 37°C

Table 4. Incident Power Density and Relative Coagulation Time for 5.5 Hour Exposure Times and Temperatures Remaining Below 37°C

Power Density Incident on Sample Container (mW/cm^2)	Relative Coagulation Time
10	0.92
10	0.92
25	1.20
25	1.10
25	0.85
25	0.85
50	0.95
50	0.98
50	1.00
100	0.95
100	1.05
100	0.91
100	0.87
280	0.94
280	1.12
280	1.00
280	1.04

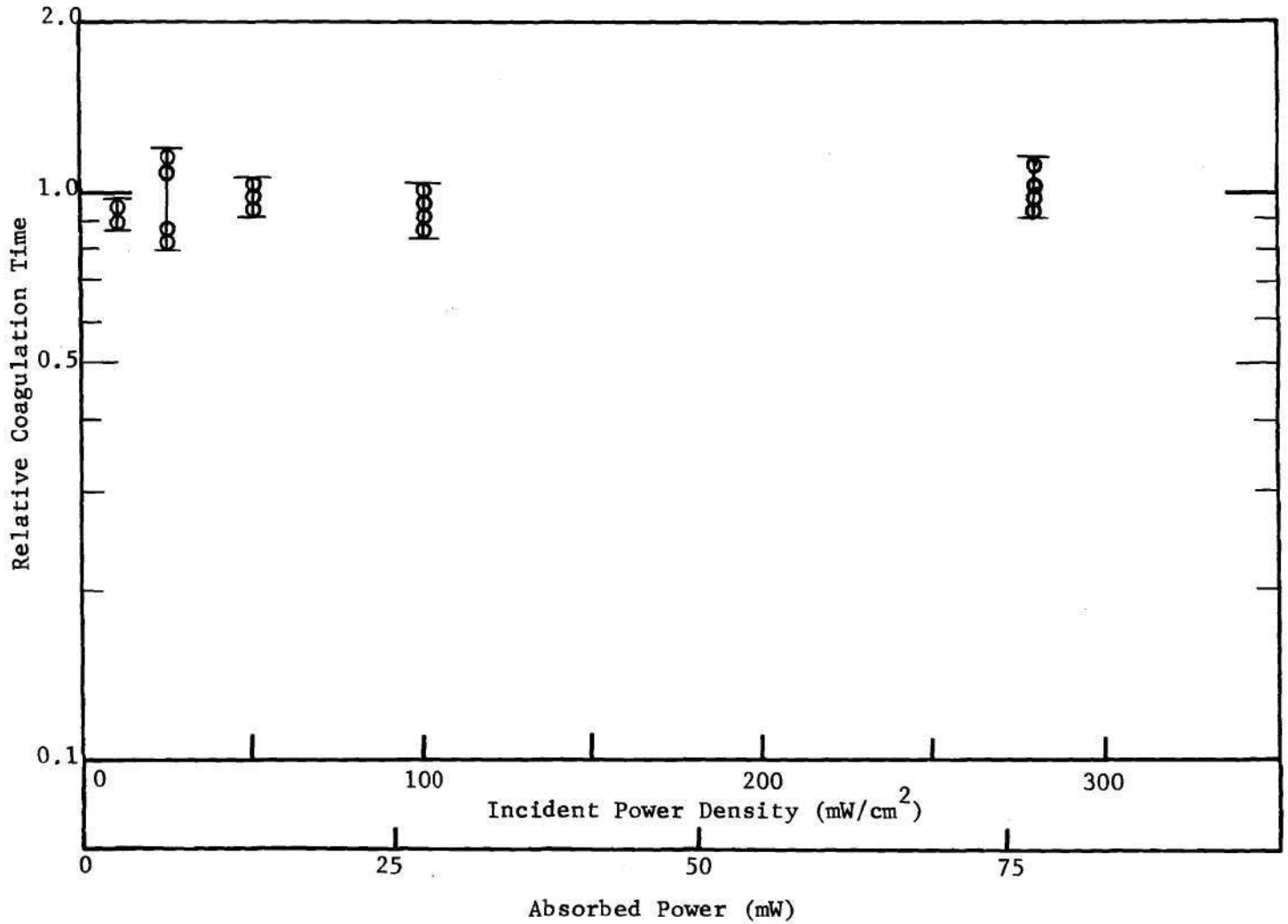

Figure 20. Relative Coagulation Time vs. Incident Power Density and Absorbed Power for 5.5 Hour Exposures and Temperatures Remaining Below 37°C

the exposure time was held constant at 5.5 hours and in all cases the plasma temperature was maintained below 37°C.

A statistical analysis of the data was performed using the procedures described in Appendix B and the results are:

$$\bar{Y} = 0.979412$$

$$Y_{rms} = 0.983999$$

$$\sigma y = 0.094898$$

$$r = 0.230437 \ .$$

The estimating equation is:

$$Y = 0.000215X + 0.956738 \ .$$

Assuming a t-distribution of the data:

$$\bar{X} = 0.97941 \pm 0.05001$$

for 95% confidence limits.

Similar results were found when comparing changes in the clot strength as a function of power densities between 10 mW/cm^2 and 280 mW/cm^2 (absorbed power of 2.7 mW to 77 mW). See Table 5 and Figure 21. No significant difference was noted. The exposure time was again constant at 5.5 hours and temperatures in the plasma remained below 37°C.

Using the procedure described in Appendix B, statistical analysis of the data produced the following:

$$\bar{Y} = 1.015000$$

$$Y_{rms} = 1.031086$$

Table 5. Incident Power Density and Relative Clot Strength for 5.5 Hour Exposure Times and Temperatures Remaining Below 37°C

Power Density Incident on Sample Container (mW/cm^2)	Relative Clot Strength
10	1.16
10	1.16
25	0.94
25	0.88
25	0.94
50	1.09
50	0.97
50	1.16
100	1.03
100	1.57
100	0.94
100	0.86
280	1.00
280	0.80
280	0.87
280	0.87

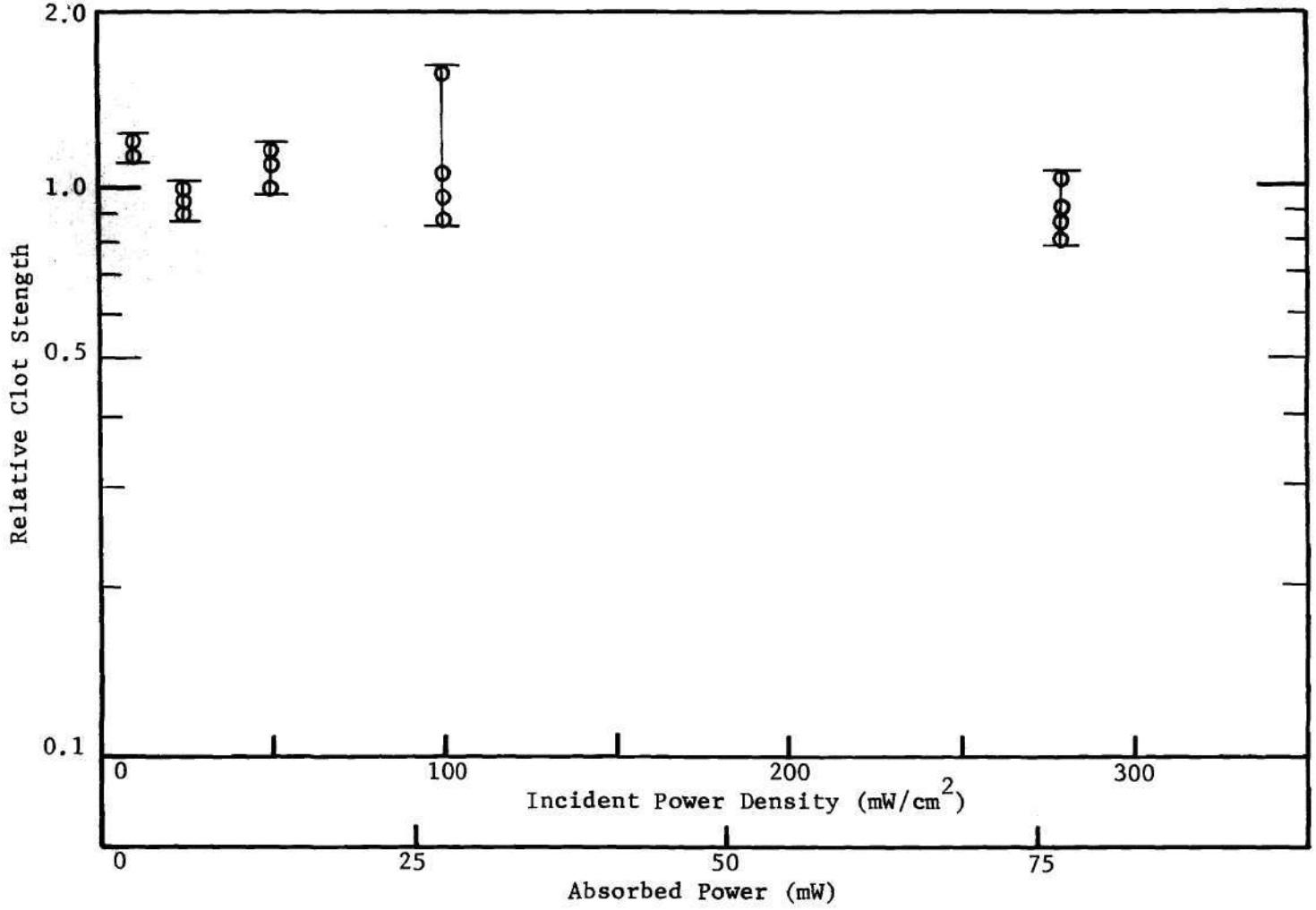

Figure 21. Relative Clot Strength vs. Incident Power Density and Absorbed Power for 5.5 Hour Exposures and Temperatures Remaining Below 37°C

$\sigma y = 0.181418$

$r = - 0.359486$

The estimating equation is:

$$Y = - 0.000636X + 1.085110 \quad .$$

Assuming a t-distribution of the data:

$$\bar{X} = 1.0100 \pm 0.09871$$

for 95% confidence limits.

The previous results show that, for constant exposure times of 5.5 hours, there is no significant change in platelet count, coagulation time and clot strength with in vitro exposures to microwave power densities between 10 mW/cm^2 and 280 mW/cm^2 when the plasma temperature remains at or below normal body temperature (37°C).

An investigation was conducted to look at the effect of varying exposure rates on the platelet count at relatively low incident power densities. The first exposures were made at 10 mW/cm^2 with the exposure times varying from 0.5 hours to 24 hours. The 24 hour maximum time was chosen since the normal platelet count begins to decrease significantly as the time after removal from the body increases beyond 24 hours. As an example, a platelet count on a sample of plasma was counted immediately after being drawn and showed 445,000 per mm^3. After retention for 24 hours at 23°C, the platelet count dropped to 293,000 per mm^3.

Table 6 and Figure 22 show the results of relative platelet count vs. exposure times of 0.5 hours to 24 hours for a constant power density of 10 mW/cm^2 and temperatures remaining below normal body

Table 6. Exposure Time and Relative Platelet Count at 10 mW/cm^2 and Temperatures Remaining Below 37°C

Exposure Time (Hours)	Relative Platelet Count
0.5	0.99
0.5	1.03
0.5	0.98
2.0	0.90
2.0	1.08
2.0	1.05
3.0	1.02
3.0	1.01
3.0	1.02
5.5	1.11
5.5	0.97
5.5	1.05
5.5	0.78
5.5	0.96
24.0	0.87
24.0	0.71
24.0	0.70
24.0	0.77
24.0	1.17
24.0	1.15
24.0	1.25

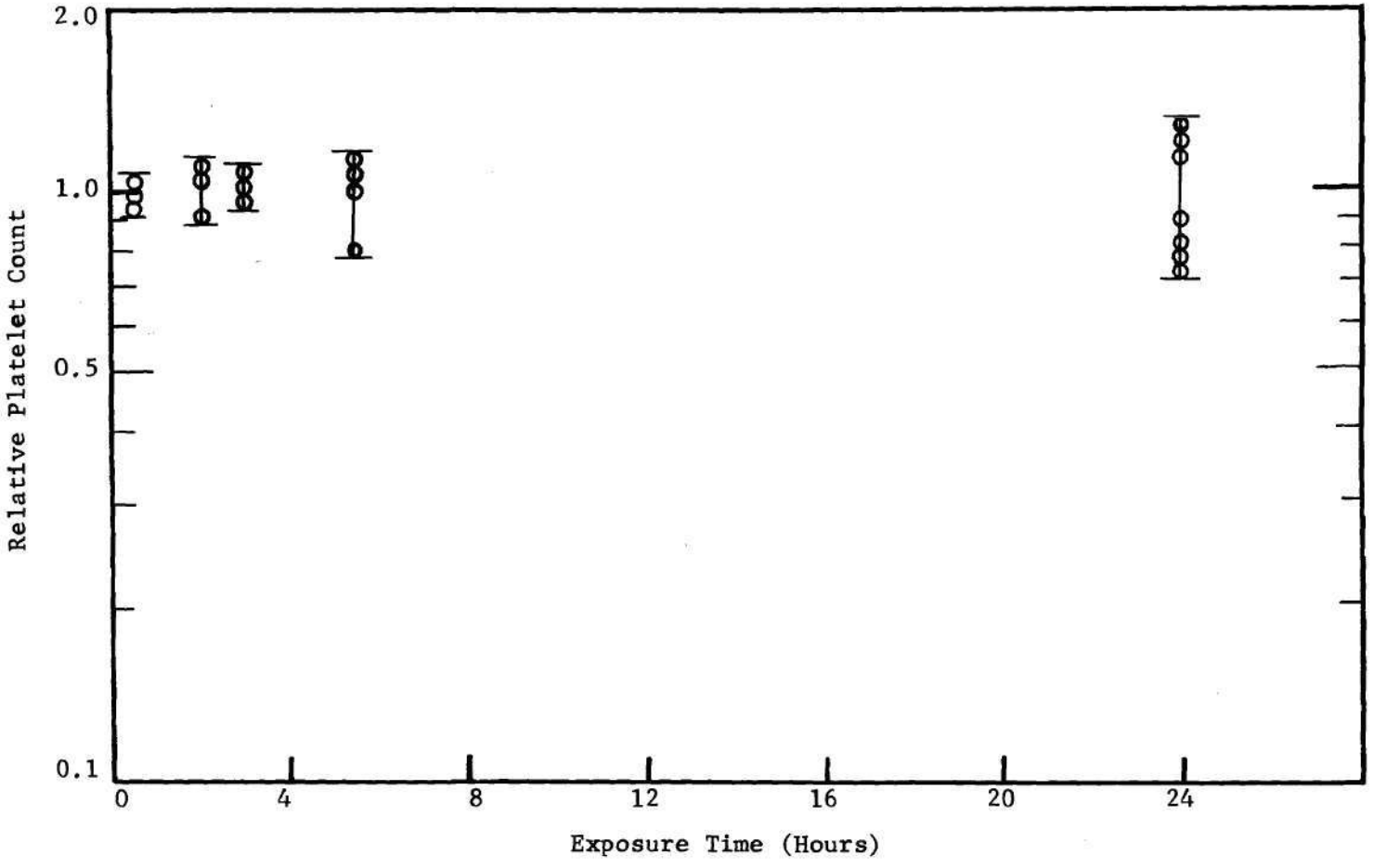

Figure 22. Relative Platelet Count vs. Exposure Time at 10 mW/cm^2 and Temperatures Remaining Below 37°C

temperature. It is apparent that there is no significant change in the platelet count over a 24 hour exposure time. The larger deviation in the 24 hour data results from the difficulty in maintaining a constant temperature of $\pm 1^{\circ}C$ in both the control sample and irradiated sample over a full 24 hours.

Following the procedure of Appendix B, the following results were obtained from an analysis of the data:

$$\bar{Y} = 0.979524$$

$$Y_{rms} = 0.990058$$

$$\sigma y = 0.144040$$

$$r = -0.175408 \quad .$$

The estimating equation is:

$$Y = -0.002537X + 1.005135 \quad .$$

Assuming a t-distribution of the data:

$$\bar{X} = 0.97952 \pm 0.06490$$

for 95% confidence limits.

Similarly, with the temperature below $37^{\circ}C$ and exposure time of 0.5 hours to 24 hours, the relative platelet count was observed for considerably higher power densities of 100 mW/cm^2 to 280 mW/cm^2. Again, as shown in Table 7 and Figure 23, no significant change was noted. The statistical analysis shows:

$$\bar{Y} = 0.966250$$

$$Y_{rms} = 1.003990$$

$$\sigma y = 0.272684$$

Table 7. Exposure Time and Relative Platelet Count at Power Densities Between 100 and 280 mW/cm^2 and Temperatures Remaining Below $37^{\circ}C$

Exposure Time (Hours)	Relative Platelet Count
0.5	1.18
0.5	1.09
0.5	1.06
0.5	0.96
0.5	1.03
3.0	1.05
3.0	0.93
5.5	1.24
5.5	1.18
5.5	1.04
5.5	0.96
5.5	0.99
5.5	0.84
5.5	0.88
5.5	0.99
5.5	0.92
5.5	0.94
24.0	0.47
24.0	0.40
24.0	0.40
24.0	0.56
24.0	1.32
24.0	1.26
24.0	1.50

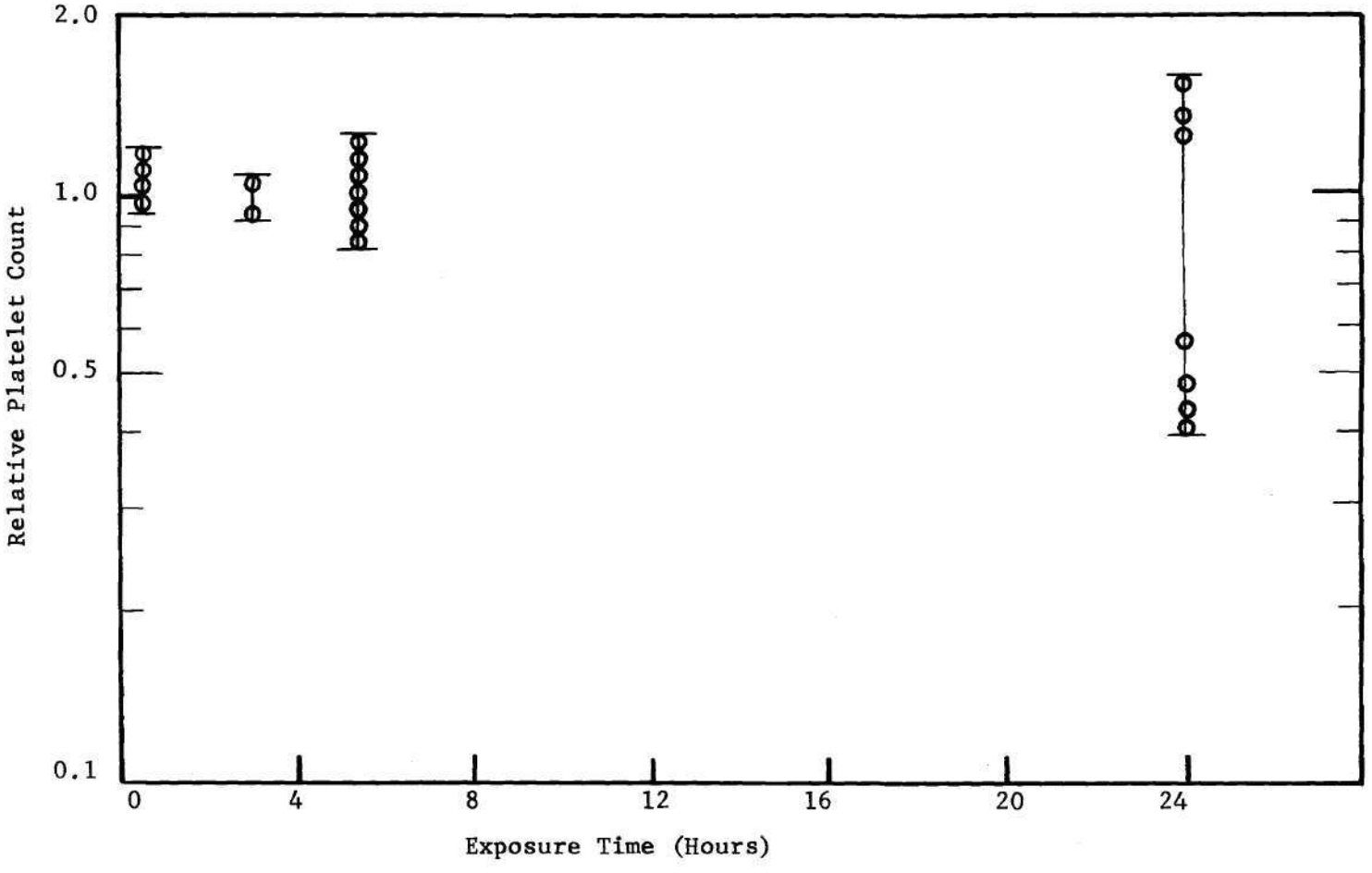

Figure 23. Relative Platelet Count vs. Exposure Time at Power Densities Between 100 and 280 mW/cm^2 and Temperatures Remaining Below 37°C

$$r = -0.298393 \ .$$

The estimating equation is:

$$Y = -0.008656X + 1.049743 \ .$$

Assuming a t-distribution of the data:

$$\bar{X} = 0.966250 \pm 0.11792$$

for 95% confidence limits.

Although it was not the expressed purpose of this research to investigate any thermal effects, an unusual observation was noted and work was done to confirm this unexpected observation. It was noted that some unexplained results were occurring to the coagulation time and clot strength of the plasma as the temperatures were increased above the normal body temperature of 37°C. While platelets were also counted in this investigation, the results are not reported because as the temperature of the plasma is increased above 37°C, the normal tendency of platelet clumping occurs and therefore a meaningful conclusion from counting unclumped platelets is not possible.

To study this observation, a control sample was maintained at 23°C and its platelet count assigned a relative factor of 1.0. A second sample was carefully maintained at a temperature rise and final temperature of that of the irradiated sample. The irradiated (third) sample was exposed to varying power densities selected to obtain a given maximum temperature rise. As previously noted, the maximum temperature was usually reached in 30 to 45 minutes. The reported data is based upon total exposure times of 5.5 hours; however, shorter exposure times showed similar, but less significant changes. Table 8 and Figure 24

Table 8. Maximum Temperature Rise and Relative Coagulation Time for Exposure Times of 5.5 Hours and Independent of Power Density

Maximum Temperature Rise (°C)	Relative Coagulation Time	
	Radiant Heating Only	Microwave Heating
34	1.11	1.16
34	1.28	1.11
34	1.00	1.00
37	0.95	1.16
37	0.76	0.76
39	1.84	1.44
39	1.69	1.10
39	1.22	1.04
42	1.70	1.10
42	2.53	1.16
42	1.87	0.96

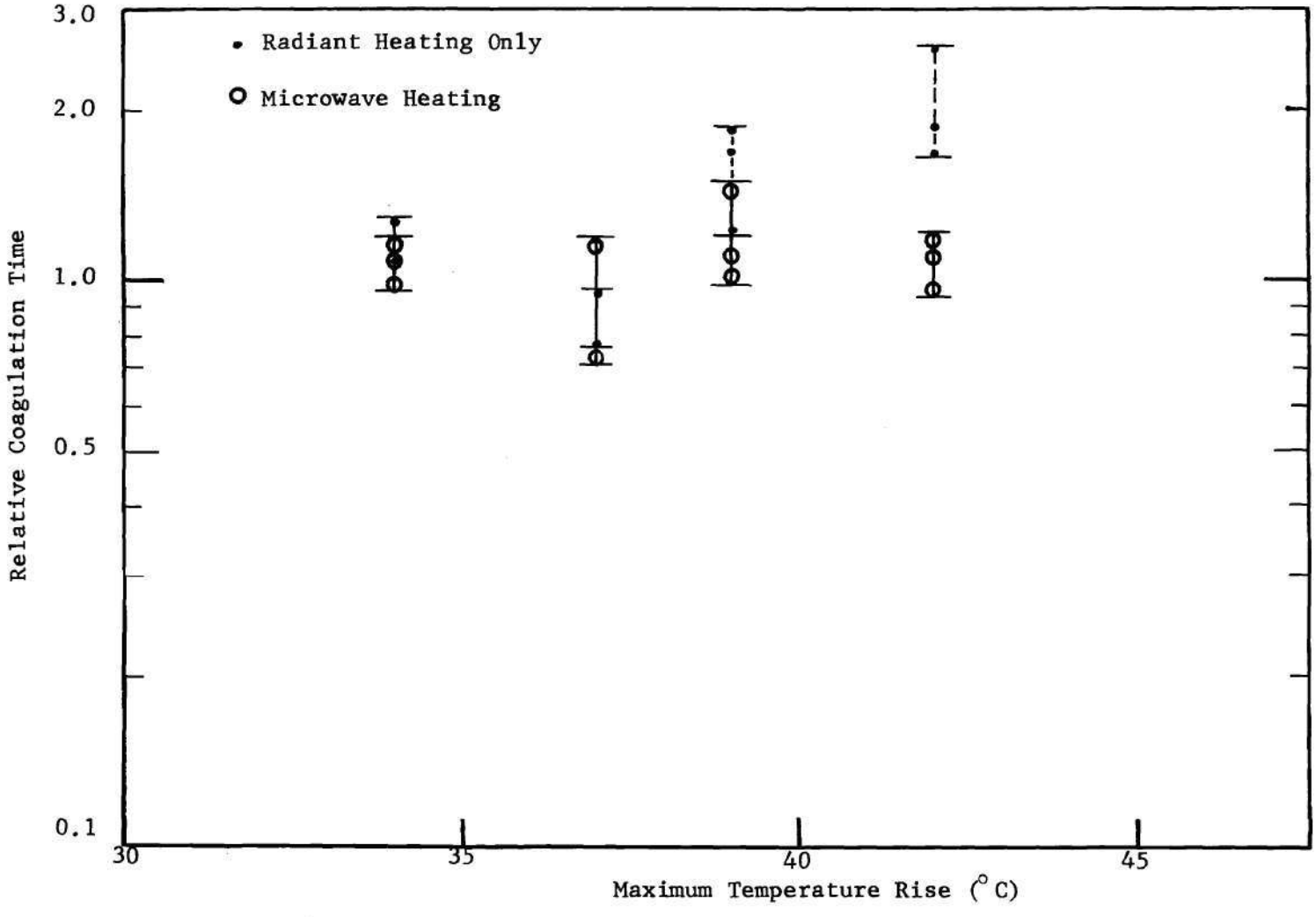

Figure 24. Relative Coagulation Time vs. Maximum Temperature Rise for Exposure Times of 5.5 Hours and Independent of Power Density

show the results of coagulation time vs. maximum temperature rise and Table 9 and Figure 25 show similar results of clot strength vs. maximum temperature rise. In each case a comparison is made at given temperatures with the relative count of the control sample to which no additional heat above room temperature (23°C) was provided.

Observation of the data clearly shows that above about 37°C, the coagulation time of the plasma increases significantly when only heat is applied to the sample. This is to be expected. However, when the same temperature is maintained as a result of microwave heating, there is a tendency for the plasma to maintain its normal coagulation time. This change is more apparent as the temperature increases above 37°C.

Using a straight line as a line of best fit for the data above 37°C, a linear regression analysis shows a slope of 0.1500 for the radiant heat data and intersecting the normalized line at 35°C. The line of best fit for the data from microwave heating shows a very small slope of - 0.0400.

The change in clot strength shows a consistently similar, but reverse effect. With a controlled temperature rise and no microwave exposure, the clot strength decreases with increasing temperature. Microwave heating tends to reduce any effect from increased temperature rise.

Linear regression analysis of the data above 37°C shows a slope of - 0.1611 for the radiant heat data and intersecting the normalized line at 38°C. As before, the data from microwave heating shows a very small slope of - 0.0511.

Table 9. Maximum Temperature Rise and Relative Clot Strength for Exposure Times of 5.5 Hours and Independent of Power Density

Maximum Temperature Rise (°C)	Relative Clot Strength	
	Radiant Heating Only	Microwave Heating
34	0.80	0.89
37	0.86	0.70
37	0.94	0.84
39	0.71	1.00
39	1.15	1.10
39	0.53	0.57
42	0.29	0.64
42	0.25	0.74
42	0.40	0.83

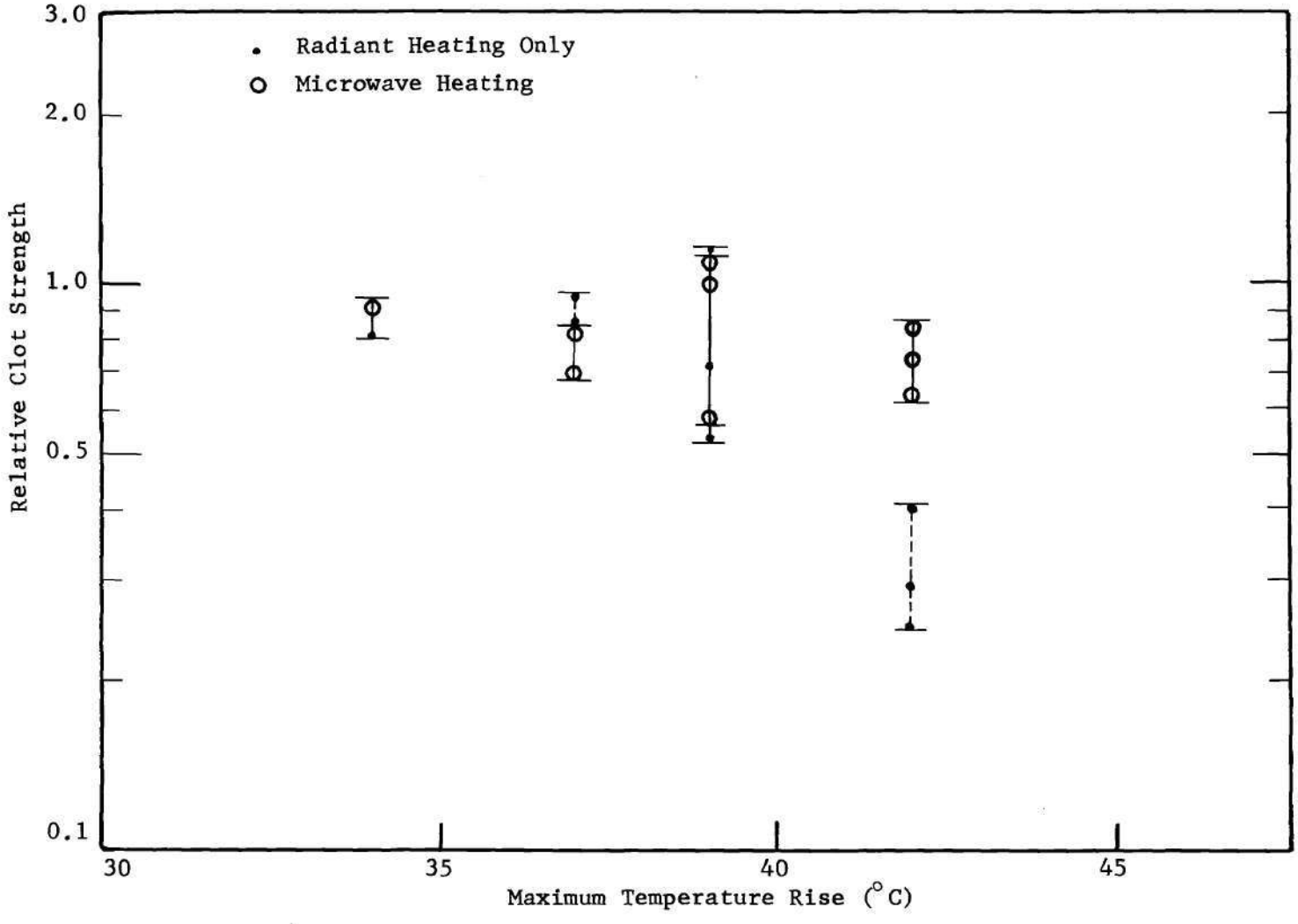

Figure 25. Relative Clot Strength vs. Maximum Temperature Rise for Exposure Times of 5.5 Hours--With Varying Power Densities of 10 mW/cm^2 to 280 mW/cm^2

Figure 26 shows a thrombelastogram of these results. The tracing on the left is from a control sample maintained at 23°C. The center curve is from the same plasma with a temperature rise of 42°C. The tracing on the right is the same plasma after being irradiated to obtain the 42°C temperature rise.

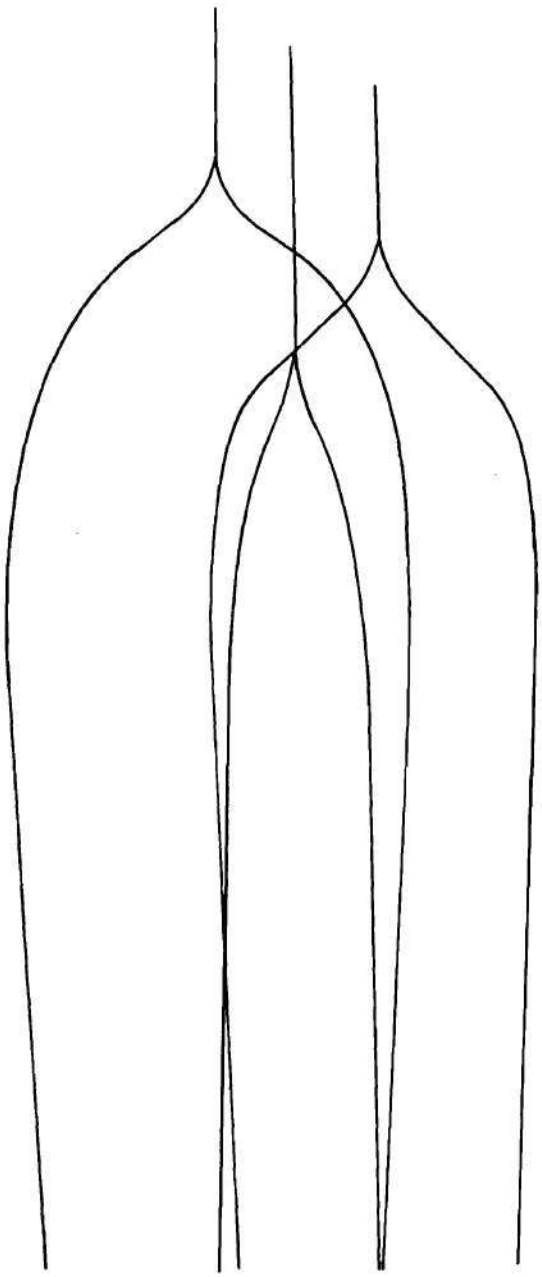

Figure 26. Thrombelastogram Showing Effects of Normal and Microwave Heating to Blood Plasma

CHAPTER VII

CONCLUSIONS AND RECOMMENDATIONS

Conclusions

One of the major purposes of this research was to design and fabricate a relatively inexpensive and compact 2450 MHz microwave irradiation system for performing precision measurements and analysis of small biological specimens. It has been shown that such a system is both possible and practical. The fabrication cost for the complete system is less than $10,000 and utilizes an area of less than 11.0 cm^2.

When performing biological studies, great care must be taken to insure that the microwave parameters are fully described and that the experimenter has confidence in his measurement of variables such as the incident power density, absorbed power, field characteristics, etc.

There is a need for greater understanding of the personnel hazards associated with the operation of microwave equipment and systems. There are no recognized or accepted radiation safety procedures to be followed when working with potentially hazardous microwave equipment.

Investigation of the non-thermal effects to human platelet-rich plasma shows that no significant changes occur to <u>in vitro</u> platelets, coagulation time or clot strength for power densities up to 280 mW/cm^2. Similarly, no effect is noticed when the exposure rates vary from continuous exposures of 0.5 hours to 24 hours at power densities between 10 mW/cm^2 and 280 mW/cm^2. This conclusion agrees with observed effects

to platelets from ionizing radiation where it has been noted that platelets are relatively "radioresistant" to ionizing radiation after they have been separated from the parent megakaryocyte.

An unexplained effect occurs when plasma temperature is raised above normal body temperature. No definite explanation can be made as to why external radiant heating in the temperature range of 37°C to 42°C (98.6°F to 105°F) produces an increase in coagulation time and decrease in clot strength whereas this is not as significantly observed when heated by microwave radiation. Additional studies should be conducted to confirm this phenomenon.

In order to produce meaningful studies on biological effects from microwave exposure, it is essential that there be close cooperation between professional disciplines.

Recommendations

Investigations on biological effects from microwave radiation must include an understanding of the microwave components and systems being used. Field characteristics, power levels, measurement techniques, etc., must be clearly defined and evaluated.

Many of the uncertainties on the biological effects previously reported appear to result from measurement errors. Standard measurement techniques and measuring equipment should be developed including standard methods for reporting results of microwave investigations.

There is a need for the development of effective and inexpensive equipment for surveying and monitoring microwave radiation at various frequencies and power densities.

Improved microwave dosimetry techniques need to be developed as soon as possible. Such techniques must be developed to evaluate conditions under both near-field and far-field characteristics.

A separate and independent study should be performed to confirm the observation noted at temperatures above 37°C in this research.

Additional investigations should be conducted on low-level effects to other biological systems such as the eye, reproductive organs, central nervous system, etc.

Educational programs should be intensified to alert workers of the potential hazards from working with microwave systems and to increase an awareness of proper radiation safety procedures.

Standardized radiation safety criteria should be developed and recognized by those employed in the microwave industry.

Additional studies need to be performed in order to effectively determine safe exposure criteria for both the general population and those occupationally employed.

APPENDICES

APPENDIX A

MULTILAYER COMPUTER PROGRAM

This multilayer computer program is based on work performed by Richmond[80] and Breeden[81] using matrix multiplication to study multilayer systems for normal incident fields. The program is written in Fortran IV language for running on the UNIVAC 1108 system at Georgia Tech.

```
  1*    C'MULTILAYER PROGRAM
  2*          DOUBLE PRECISION D(5),ER(5),TD(5),F,E1,E2,E3,TD1,TD2,TD3,D1,D2,D3
  3*    C'F MUST BE EXPRESSED IN GHZ AND IN DBL PRECISION> E.G., 2.41D0 (DEF ZERO)
  4*          DATA F/2.45D0/
  5*    C'RELATIVE DIEL CONSTANT OF EACH LAYER (E1,E2,E3) MUST BE EXPRESSED IN
  6*    C DOUBLE PRECISION ALSO.
  7*          DATA E1/4.2D0/
  8*          DATA E2/64.0D0/
  9*          DATA E3/4.2D0/
 10*    C'LOSS TANGENT OF EACH LAYER (TD1,TD2,TD3) ALSO IN DBL PRECN.
 11*          DATA TD1/.005D0/
 12*          DATA TD2/0.30D0/
 13*          DATA TD3/.005D0/
 14*    C'N IS THE NUMBER OF LAYERS (AN INTEGER)
 15*          DATA N/3/
 16*    C'D1,D2,D3 ARE THICKNESSES OF LAYERS IN INCHES> DOUBLE PRECISION.
 17*          DATA D1/.105D0/
 18*          DATA D2/.590D0/
 19*          DATA D3/.105D0/
 20*          D(1)=D1
 21*          D(2)=D2
 22*          D(3)=D3
 23*          ER(1)=E1
 24*          ER(2)=E2
 25*          ER(3)=E3
 26*          TD(1)=TD1
 27*          TD(2)=TD2
 28*          TD(3)=TD3
 29*          CALL MULTLY(N,D,ER,TD,F,ATN2M2,ARC2M2)
 30*          PXMIT=ATN2M2*100.
 31*          PREFL=ARC2M2*100.
 32*          PABSB=100.-PXMIT-PREFL
 33*    C'PXMIT=PERCENT OF INCIDENT POWER TRANSMITTED
 34*    C'PREFL=          'D0'              REFLECTED
 35*    C'PABS=           'D0'              ABSORBED BY ENTIRE STRUCTURE. FOR HIGH
 36*    C    LOSS TANGENT SAMPLE, ASSUME ALL POWER ABSORBED IN SAMPLE ITSELF. NONE
 37*    C    IN WALLS HOLDING THE SAMPLE.
 38*           WRITE(6,5) (ER(I),I=1,3),(TD(I),I=1,3),(D(I),I=1,3),PREFL,PXMIT,
 39*          2 PABSB
 40*         5 FORMAT(1H1,35X,31HLAYER 1     LAYER 2     LAYER 3//30H RELATIVE DI
 41*          2ELECTRIC CONSTANT:,3F12.4/17X,13HLOSS TANGENT:,3F12.4/10X,20HTHICK
 42*          3NESS IN INCHES:,3F12.5////13X,37HPERCENT OF INCIDENT POWER REFLECT
 43*          4ED= ,F8.5/11X,39HPERCENT OF INCIDENT POWER TRANSMITTED= ,F8.5/50H
 44*          5PERCENT OF INCIDENT POWER ABSORBED BY STRUCTURE= ,F8.5////)
 45*           STOP
 46*           END
```

```
1*          SUBROUTINE MULTLY(N,D,ER,TD,F,ATN2M2,ARC2M2)
2*    C ATN2M2=POWER TRANSMISSION COEF FOR N LAYER STRUCTURE (SINGLE PRECISION)
3*    C ARC2M2=POWER REFLECTION COEF FOR N LAYER STRUCTURE (SINGLE PRECISION)
4*    C PROGRAM GOOD FOR NORMAL INCIDENCE ONLY
5*          DOUBLE PRECISION D(5),ER(5),TD(5),PI,TUPI,F,RE(5),IE(5),RG(5),IG(5
6*         1),RR2(5),IR2(5),DD,WL,AB,SR,GG,TP,RRR2,IRR2,RA2,IA2
7*         2,RY1,IY1,RY2,IY2,RY3,IY3,RY4,IY4,RV1,IV1,RV2,IV2,RV3,IV3,RV4,IV4,R
8*         3Q1,IQ1,RQ2,IQ2,RQ3,IQ3,RQ4,IQ4,RRC2,IRC2,RC2M,RC2M2,RTN2,ITN2,TN2M
9*         4,TN2M2,RTD,PR2,XX2,APD2,TP1,TP2,TP3,TP4,TP5,TP6
10*     208 FORMAT(//13X,7HCOMPLEX,30X,7HCOMPLEX,24X,5HPOWER,9X,5HPOWER/4X,24H
11*        1TRANSMISSION COEFFICIENT,15X,22HREFLECTION COEFFICIENT,12X,25HTRAN
12*        2SMISSION   REFLECTION,12X,9HINSERTION/4X,120HREAL      IMAG   MAGNI
13*        3TUDE  ANGLE      REAL      IMAG   MAGNITUDE  ANGLE    COEFFICIENT
14*        4COEFFICIENT              PHASE DELAY/)
15*     209 FORMAT(1X,3F9.6,F9.3,1X,3F9.6,F9.3,4X,F9.6,5X,F9.6,2F14.3)
16*          PI = 3.14159265358979324D0
17*          TUPI = 2.0D0*PI
18*          NN = N+1
19*          DO 50 I=1,N
20*          RE(I) = ER(I)
21*       50 IE(I) = -ER(I)*TD(I)
22*          ER(NN) = 1.0D0
23*          TD(NN) = 0.0D0
24*          RE(NN) = 1.0D0
25*          IE(NN) = 0.0D0
26*          DD = 0.0D0
27*          DO 75 I=1,N
28*       75 DD = DD+D(I)
29*          DD = TUPI*DD
30*          WL = 29.97925D0/F
31*          AB = (TUPI/WL)/DSQRT(2.0D0)
32*          SR = DSQRT(ER(1)**2+(ER(1)*TD(1))**2)
33*          TP1 = SR-ER(1)
34*          TP2 = SR+ER(1)
35*          IF (TP1) 76,76,77
36*       76 RG(1) = 0.0D0
37*          GO TO 78
38*       77 RG(1) = AB*DSQRT(TP1)
39*       78 IG(1) = AB*DSQRT(TP2)
40*          GG = TUPI/WL
41*          TP = (RG(1)-IE(1)*GG)**2+(IG(1)+RE(1)*GG)**2
42*          RRR2 = ((RG(1)+IE(1)*GG)*(RG(1)-IE(1)*GG)+(IG(1)-RE(1)*GG)*(IG(1)+
43*         1RE(1)*GG))/TP
44*          IRR2 = ((IG(1)-RE(1)*GG)*(RG(1)-IE(1)*GG)-(RG(1)+IE(1)*GG)*(IG(1)+
45*         1RE(1)*GG))/TP
46*          DO 84 I=1,N
47*          II = I+1
48*          SR = DSQRT(ER(II)**2+(ER(II)*TD(II))**2)
49*          TP5 = SR-ER(II)
50*          TP6 = SR+ER(II)
51*          IF (TP5) 79,79,80
52*       79 RG(II) = 0.0D0
53*          GO TO 81
54*       80 RG(II) = AB*DSQRT(TP5)
55*       81 IG(II) = AB*DSQRT(TP6)
56*          TP1 = (RE(I)*RG(II)-IE(I)*IG(II))-(RE(II)*RG(I)-IE(II)*IG(I))
57*          TP2 = (RE(I)*RG(II)-IE(I)*IG(II))+(RE(II)*RG(I)-IE(II)*IG(I))
58*          TP3 = (IE(I)*RG(II)+RE(I)*IG(II))-(IE(II)*RG(I)+RE(II)*IG(I))
59*          TP4 = (IE(I)*RG(II)+RE(I)*IG(II))+(IE(II)*RG(I)+RE(II)*IG(I))
60*          TP = TP2**2+TP4**2
61*          RR2(I) = (TP1*TP2+TP3*TP4)/TP
62*          IR2(I) = (TP3*TP2-TP1*TP4)/TP
63*       84 CONTINUE
64*          RA2 = 1.0D0-RRR2
65*          IA2 = -IRR2
66*          DO 85 I=1,N
```

```
67*          RA2 = RA2*(1.0D0-RR2(I))+IA2*IR2(I)
68*       85 IA2 = IA2*(1.0D0-RR2(I))-RA2*IR2(I)
69*          TP = RA2**2+IA2**2
70*          RA2 = RA2/TP
71*          IA2 = -IA2/TP
72*          RY1 = DEXP(-D(1)*RG(1))*DCOS(D(1)*IG(1))
73*          IY1 = -DEXP(-D(1)*RG(1))*DSIN(D(1)*IG(1))
74*          RY4 = DEXP(D(1)*RG(1))*DCOS(D(1)*IG(1))
75*          IY4 = DEXP(D(1)*RG(1))*DSIN(D(1)*IG(1))
76*          RY2 = -(RRR2*RY4-IRR2*IY4)
77*          IY2 = -(IRR2*RY4+RRR2*IY4)
78*          RY3 = -(RRR2*RY1-IRR2*IY1)
79*          IY3 = -(IRR2*RY1+RRR2*IY1)
80*          DO 105 I=2,NN
81*          IF (I-NN) 95,90,90
82*       90 RV1 = 1.0D0
83*          IV1 = 0.0D0
84*          RV2 = -RR2(N)
85*          IV2 = -IR2(N)
86*          RV3 = -RR2(N)
87*          IV3 = -IR2(N)
88*          RV4 = 1.0D0
89*          IV4 = 0.0D0
90*          GO TO 100
91*       95 II = I-1
92*          RV1 = DEXP(-D(I)*RG(I))*DCOS(D(I)*IG(I))
93*          IV1 = -DEXP(-D(I)*RG(I))*DSIN(D(I)*IG(I))
94*          RV4 = DEXP(D(I)*RG(I))*DCOS(D(I)*IG(I))
95*          IV4 = DEXP(D(I)*RG(I))*DSIN(D(I)*IG(I))
96*          RV2 = -(RR2(II)*RV4-IR2(II)*IV4)
97*          IV2 = -(IR2(II)*RV4+RR2(II)*IV4)
98*          RV3 = -(RR2(II)*RV1-IR2(II)*IV1)
99*          IV3 = -(IR2(II)*RV1+RR2(II)*IV1)
100*     100 RQ1 = (RY1*RV1-IY1*IV1)+(RY2*RV3-IY2*IV3)
101*         IQ1 = (IY1*RV1+RY1*IV1)+(IY2*RV3+RY2*IV3)
102*         RQ2 = (RY1*RV2-IY1*IV2)+(RY2*RV4-IY2*IV4)
103*         IQ2 = (IY1*RV2+RY1*IV2)+(IY2*RV4+RY2*IV4)
104*         RQ3 = (RY3*RV1-IY3*IV1)+(RY4*RV3-IY4*IV3)
105*         IQ3 = (IY3*RV1+RY3*IV1)+(IY4*RV3+RY4*IV3)
106*         RQ4 = (RY3*RV2-IY3*IV2)+(RY4*RV4-IY4*IV4)
107*         IQ4 = (IY3*RV2+RY3*IV2)+(IY4*RV4+RY4*IV4)
108*         RY1 = RQ1
109*         IY1 = IQ1
110*         RY2 = RQ2
111*         IY2 = IQ2
112*         RY3 = RQ3
113*         IY3 = IQ3
114*         RY4 = RQ4
115*     105 IY4 = IQ4
116*         TP = RY4**2+IY4**2
117*         RRC2 = -(RY3*RY4+IY3*IY4)/TP
118*         IRC2 = -(IY3*RY4-RY3*IY4)/TP
119*         RC2M = DSQRT(RRC2**2+IRC2**2)
120*         RTN2 = (RY1+(RY2*RRC2-IY2*IPC2))*RA2-(IY1+(IY2*RRC2+RY2*IRC2),*IA2
121*         ITN2 = (IY1+(IY2*RRC2+RY2*IRC2))*RA2+(RY1+(RY2*RRC2-IY2*IRC2),*IA2
122*         TN2M = DSQRT(RTN2**2+ITN2**2)
123*         RC2M2 = RC2M*RC2M
124*         TN2M2 = TN2M*TN2M
125*         RTD = 180.0D0/PI
126*         IF (RRC2) 115,116,117
```

```
127*      115 PR2 = RTD*(PI+DATAN(IRC2/RRC2))
128*          GO TO 118
129*      116 PR2 = DSIGN(RTD*(PI/2.0D0),IRC2)
130*          GO TO 118
131*      117 PR2 = RTD*DMOD((TUPI+DATAN(IRC2/PRC2)),TUPI)
132*      118 CONTINUE
133*          IF (RTN2) 125,126,127
134*      125 XX2 = RTD*(PI+DATAN(ITN2/RTN2))
135*          GO TO 128
136*      126 XX2 = DSIGN(RTD*(PI/2.0D0),ITN2)
137*          GO TO 128
138*      127 XX2 = RTD*DMOD((TUPI+DATAN(ITN2/RTN2)),TUPI)
139*      128 CONTINUE
140*          APD2 = -(RTD*(DD/WL)+XX2)
141*          ATN2M = SNGL(TN2M)
142*          AXX2 = SNGL(XX2)
143*          ARC2M = SNGL(RC2M)
144*          APR2 = SNGL(PR2)
145*          ATN2M2 = SNGL(TN2M2)
146*          ARC2M2 = SNGL(RC2M2)
147*          AAPD2 = SNGL(APD2)
148*          ARTN2 = SNGL(RTN2)
149*          AITN2 = SNGL(ITN2)
150*          ARRC2 = SNGL(RRC2)
151*          AIRC2 = SNGL(IRC2)
152*          IF (ABS(AAPD2).GT.360.) GO TO 129
153*          CPD = 360.+AAPD2
154*          GO TO 130
155*      129 CPD = 720.+AAPD2
156*      130 CONTINUE
157*          RETURN
158*          END
```

	LAYER 1	LAYER 2	LAYER 3
RELATIVE DIELECTRIC CONSTANT:	4.2000	64.0000	4.2000
LOSS TANGENT:	.0050	.3000	.0050
THICKNESS IN INCHES:	.10500	.59000	.10500

PERCENT OF INCIDENT POWER REFLECTED= 67.27878
PERCENT OF INCIDENT POWER TRANSMITTED= 8.54861
PERCENT OF INCIDENT POWER ABSORBED BY STRUCTURE= 24.17261

APPENDIX B

STATISTICAL ANALYSIS

Statistical analysis of data shown in Table 3 and Figure 19, including Linear Regression with Means, RMS Values, Variances, Correlation Coefficient and t-Distribution.

The linear regression fits a curve of the form $Y = mX + b$ where m is the slope and b is the Y intercept.

X	Y	X^2	Y^2	XY
10	1.11	100	1.232	11.10
10	0.97	100	0.941	9.70
10	1.05	100	1.103	10.50
10	0.78	100	0.608	7.80
10	1.16	100	1.346	11.60
25	1.09	625	1.188	27.25
25	1.08	625	1.166	27.00
25	0.90	625	0.810	22.50
25	0.92	625	0.846	23.00
50	0.96	2,500	0.922	48.00
50	0.97	2,500	0.941	48.50
50	0.88	2,500	0.774	44.00
60	0.99	3,600	0.980	59.40
60	0.95	3,600	0.903	57.00
100	1.24	10,000	1.538	124.00
100	1.18	10,000	1.392	118.00
100	0.99	10,000	0.980	99.00
100	0.84	10,000	0.706	84.00
100	0.88	10,000	0.774	88.00
100	0.99	10,000	0.980	99.00
100	0.92	10,000	0.846	92.00
100	0.94	10,000	0.884	94.00
280	1.04	78,400	1.082	291.20
280	0.95	78,400	0.903	266.00
280	1.18	78,400	1.392	330.40
280	1.09	78,400	1.188	305.20
2340	26.05	411,300	26.425	2398.15

Arithmetic Mean

$$\bar{Y} = \frac{\Sigma Y}{N} = \frac{26.05}{26}$$

$$\bar{Y} = 1.0019$$

$$\bar{X} = \frac{\Sigma X}{N} = \frac{2340}{N}$$

$$\bar{X} = 90.000$$

RMS Values

$$Y_{rms} = \sqrt{\overline{Y^2}} = \sqrt{\frac{\Sigma Y^2}{N}}$$

$$= \frac{26.425}{26}$$

$$Y_{rms} = 1.0081$$

$$X_{rms} = \sqrt{\overline{X^2}} = \sqrt{\frac{\Sigma X^2}{N}}$$

$$= \frac{411,300}{26}$$

$$X_{rms} = 125.7745$$

Standard Deviation. This is a measure of the spread or dispersion of the distribution of data.

$$\sigma y = \sqrt{\overline{Y^2} - (\bar{Y})^2}$$

$$= 1.01635 - 1.00385$$

$$\sigma y = 0.1118$$

$$\sigma X = \sqrt{\overline{X^2} - (\bar{X})^2}$$

$$= 15819.231 - 8100$$

$$\sigma X = 87.8591$$

Linear Regression. This is a calculation of an equation of the straight line of best fit of a set of data. It is determined by minimizing the sum of the squares of the deviations of the data points from the line. It determines an estimating equation $Y = mX + b$ where m, the slope, indicates by its sign the direction of the slope (and whether the correlation is positive or negative) and by its value the amount of change in the Y series for each unit change in the X series. b is the Y intercept, the value where the estimating equation intersects the Y axis when X is zero.

Slope

$$m = \frac{\Sigma(X_i - \bar{X})(Y_i - \bar{Y})}{\Sigma(X_i - \bar{X})^2}$$

$$= \frac{\overline{XY} - \bar{X}\,\bar{Y}}{(\sigma X)^2}$$

$$= \frac{92.237 - 90.173}{(87.8591)^2}$$

$$m = 0.000267$$

Y Intercept

$$b = \bar{Y} - m\bar{X}$$

$$= 1.001923 - (0.000267)(90.0)$$

$$b = 0.97786$$

Correlation Coefficient. This determines the degree of association between variables (both positive and negative) with zero indicating no association and ± 1 indicating perfect correlation.

$$r = \frac{\Sigma(X_i - \bar{X})(Y_i - \bar{Y})}{\sqrt{\Sigma(X_i - \bar{X})^2 \, \Sigma(Y_i - \bar{Y})^2}}$$

$$= \frac{N\Sigma XY - \Sigma X \Sigma Y}{\sqrt{[N\Sigma X^2 - (\Sigma X)^2][N\Sigma Y^2 - (\Sigma Y)^2]}}$$

$$= \frac{m\,\sigma X}{\sigma Y}$$

$$= \frac{(0.000267)(87.8591)}{0.1118}$$

$$r = 0.2102$$

t-Distribution. This provides a measure of the signifcance of difference between the means and an estimated means, and approaches the normal curve when the degrees of freedom approaches 20. Statistically, it casts much or little doubt on a hypothesis. Using a t-distribution to examine the data, one can compare the mean relative values of the irradiated samples to the normalized value of the controls and determine if there is a significant change.

Relative Platelet Count	f	d'	fd'	$f(d')^2$
1.11	1	+0.11	+0.11	0.0121
0.97	2	-0.03	-0.06	0.0018
1.05	1	+0.05	+0.05	0.0025
0.78	1	-0.22	-0.22	0.0484
1.16	1	+0.16	+0.16	0.0256
1.09	2	+0.09	+0.18	0.0162
1.08	1	+0.08	+0.08	0.0064
0.90	1	-0.10	-0.10	0.0100
0.92	2	-0.08	-0.16	0.0128
0.96	1	-0.04	-0.04	0.0016
0.88	2	-0.12	-0.24	0.0288
0.99	3	-0.01	-0.03	0.0003
0.95	2	-0.05	-0.10	0.0050
1.24	1	+0.24	+0.24	0.0576
1.18	2	+0.18	+0.36	0.0648
0.84	1	-0.16	-0.16	0.0256
0.94	1	-0.06	-0.06	0.0036
1.04	1	+0.04	+0.04	0.0016
	26.0		+0.05	0.3247

where:

f = frequency of occurrence

d' = deviation from expected value, $\bar{X}d$.

The arithmetic mean, $\bar{X}$:

$$\bar{X} = \bar{X}d + \frac{\Sigma fd'}{N} i$$

where:

i = class interval

$$\bar{X} = 1.0 + \frac{0.05}{26.0} (1.0)$$

$$\bar{X} = 1.00192 \quad .$$

To estimate the standard deviation σ:

$$\hat{\sigma} = i \sqrt{\frac{\Sigma f(d')^2}{N-1} - \frac{(\Sigma fd')^2}{N(N-1)}}$$

$$= 1.0\sqrt{\frac{0.3247}{25.0} - \frac{0.0025}{650.0}}$$

$$\hat{\sigma} = 0.113948 \quad .$$

To estimate the standard error of $\bar{X}$:

$$\hat{\sigma}_{\bar{X}} = \frac{\sigma}{N}$$

$$= \frac{0.113948}{26.0}$$

$$\hat{\sigma}_{\bar{X}} = 0.022347$$

Using the $\hat{\sigma}_{\bar{X}}$ and values from a "t" table for percentage points, the 95 percent confidence limits are determined.

$$\bar{X} = 1.00192 \pm 0.02347 \ (2.056)$$

$$\bar{X} = 1.00192 \pm 0.04595$$

Thus for 95 percent confidence limits $\bar{X}$ has the range of 0.95597 to 1.04787 which encompasses the normalized control value of 1.00.

BIBLIOGRAPHY

1. Okress, E. C., Microwave Power Engineering, Vol. 2, Academic Press, New York (1968)

2. Terrill, J. G., Jr., Testimony on Radiation Control for Health and Safety Act of 1967 before the Committee on Commerce, United States Senate, Part 2, May 6, 1968 (Serial No. 90-49)

3. Daily, L. E., "Clinical Study of Results of Exposure of Laboratory Personnel to Radar and High Frequency Radio," U.S. Navy Medical Bulletin, 41: 1052, (1943)

4. Daily, L., Jr., Wakim, K. G., Herrick, J. P., and Parkhill, E. M., "Effect of Microwave Diathermy on the Eyes," American Journal of Physiology, 155: 432, (1948)

5. Richardson, A. W., Duane, T. D., and Hines, H. M., "Experimental Lenticular Opacities Produced by Microwave Irradiations," Arch. Phys. Med., 29: 765, (1948)

6. Boysen, J. E., "Hyperthermic and Pathologic Effects of Electromagnetic Radiation (350 Mc)," A.M.A. Arch. Indust. Hyg., 7: 516, (1955)

7. Hirsh, F. G. and Parker, J. T., "Bilateral Lenticular Opacities Occurring in a Technician Operating a Microwave Generator," A.M.A. Arch. Indust. Hyg., 6: 512, (1952)

8. Pattishall, E. G., Proceedings of Tri-Service Conference on Biological Hazards of Microwave Radiation, University of Virginia, (1957)

9. Pattishall, E. G., and Banghart, F. W., Proceedings of Second Tri-Service Conference on Biological Effects of Microwave Energy, University of Virginia, ASTIA Doc. No. Ad-131-477, (1958)

10. Susskind, C., Proceedings of the Third Annual Tri-Service Conference on Biological Effects of Microwave Radiating Equipment, University of California, Berkeley, Calif., (1959)

11. Peyton, M. F., Proceedings of the Fourth Annual Tri-Service Conference on the Biological Effects of Microwave Radiation, Plenum Press, N. Y. (1961)

12. Schwan, H. P. and Li, K., "Hazards Due to Total Body Irradiation by Radar," Proc. IRE 44, 1572 (1956)

13. Schwan, H. P. and Li, K., "The Mechanism of Absorption of Ultrahigh Frequency Electromagnetic Energy in Tissues as Related to the Problem of Tolerance Dosage," IRE Trans. Med. Electron. Vol. PGME-4, 45, (1956)

14. Moore, W., Jr., "Biological Aspects of Microwave Radiation--A Review of Hazards," USDHEW, Public Health Service Report TSB - 4 (1968)

15. Schwan, H. P., "Radiation Biology, Medical Applications and Radiation Hazards," Microwave Power Engineering, Vol. 2, 215, Academic Press, New York (1968)

16. Drogichina, E. A. and Sadghikova, M. N., "Clinical Syndromes Arising Under the Effect of Various Radio Frequency Bands," Labor. Hyg. Occupational Diseases, Moscow, Vol. 9: 17 (1965)

17. Gordon, Z. W., "The Problem of the Biological Action of UHF," Nauchn. Issled. Inst. Hygiene Truda i Profzabolevanily; Tr., Vol. 1: 5, (1960)

18. Gordon, Z. W., "Hygiene-Probleme der Arbeit mit Zentimeterwellen-Generatoren," J. Hyg. Epidemiol. Microbiol. Immunol., Vol. 1: 472, (1957)

19. Presman, A. S., "Problem of the Mechanism of the Biological Effect of Microwaves," Progr. Mod. Biol. Moscow, Vol. 56: 161, (1963)

20. Letavet, A. A. and Gordon, Z. W., "The Biological Action of Ultra-high Frequencies," Institute of Labor Hygiene and Occupational Diseases, Academy of Medical Sciences, USSR, (1960)

21. Cleary, S. F., "Considerations in the Evaluation of the Biological Effects of Exposure to Microwave Radiation," Amer. Ind. Hyg. Assn. Journal, Vol. 31: 52, (1970)

22. White, H. E., Modern College Physics, D. Van Nostrand Co., Princeton, N. J., 271, (1956)

23. Hogness, T. R. and Johnson, W. C., Qualitative Analysis and Chemical Equilibrium, Henry Holt Co., N. Y., 36, (1940)

24. Schwan, H. P., "Radiation Biology, Medical Applications, and Radiation Hazards," Microwave Power Engineering, 2: 215, Academic Press, N. Y., (1968)

25. Ely, T. S., and Goldman, D. E., "Heating Characteristics of Laboratory Animals Exposed to Ten-Centimeter Microwaves," Proceedings of Tri-Service Conference on Biological Hazards of Microwave Radiation, University of Virginia, (1957)

26. Ely, T. S. and Goldman, E. D., "Heating Characteristics of Laboratory Animals Exposed to Ten-Centimeter Microwaves," Research Report (Project NM001 056.13.02), Naval Medical Research Institute, Bethesda, Md., Vol. 15; 77, (1957)

27. Michaelson, S. M., Howland, J. W., Thomson, R. A. E. and Mermagen, H., "Comparison of Responses to 2800 Mc and 200 Mc Microwaves or Increased Environmental Temperature, Proceedings of Third Tri-Service Conference on Biological Effects of Microwave Radiating Equipment, RADC-TR-59-140

28. Michaelson, S. M., Thomson, R. A. E., and Howland, J. W., "Biologic Effects of Microwave Exposure," Technical Report No. RACD-TR-67-461, University of Rochester, Rochester, N. Y., (1967)

29. Hoeft, L. O., "Microwave Heating, A Study of the Critical Exposure Variables for Man and Experimental Animals," Report AMRL-TR-64-127, Aerospace Medical Research Laboratories, Wright-Patterson AFB, Ohio, (1965)

30. Zaret, M. M., "Ocular Effects of Microwave Radiation," Annual Progress Report, Sept. 1966-June 1967, Grant DA-MD-49-193-67-G9224, The Zaret Foundation, Inc., Scarsdale, N. Y.

31. Hirsch, F. G. and Parker, J. T., "Bilateral Lenticular Opacities Occurring in a Technician Operating a Microwave Generator," A.M.A. Arch. Indust. Hyg. 6: 512, (1952)

32. Zaret, M. M., "Opthalmic Hazards of Microwave and Laser Environments," Annual Progress Report, June 1966- May 1967, Contract DA-49-193-MD-2592, The Zaret Foundation, Inc., Scarsdale, N.Y.

33. Zaret, M. M., "Ocular Effects of Microwave Radiation," Annual Progress Report, Sept. 1965-Sept. 1966, Grant DA-MD-49-193-66-6188, The Zaret Foundation, Inc., Scarsdale, N. Y.

34. Williams, D. B., Monahan, J. P., Nicholson, W. J., and Aldrich, J. J., "Biologic Effects Studies on Microwave Radiation Time and Power Thresholds for Production of Lens Opacities by 12.3 cm Microwaves," A.M.A. Arch. Ophth., 54: 863, (1955)

35. Daily, L., Jr., Zeller, E. A., Walkim, K., Herrick, Jr., and Benedict, W., "Influence of Microwaves upon Certain Enzyme Systems in the Lens," Am. J. Ophth., 34: 1301, (1951)

36. Seth, H. S. and Michaelson, S. M., "Microwave Cataractogenesis," J. Occup. Med., 7(9): 439, (1965)

37. Van Ummersen, C. A. and Cogan, F. C., "Experimental Microwave Cataracts, Age as Factor in Induction of Cataracts in the Rabbit," Arch. Environ. Health., 11: 177, (1965)

38. Zaret, M. M., "An Experimental Study of the Cataractogenic Effects of Microwave Radiation," Technical Documentary Report No. RADC-TDR-64-273, Rome Air Development Center, Griffiss AFB, N. Y., (1964)

39. Carpenter, R. L., "Review of the Work Conducted at Tufts University," Proceedings of Second Tri-Service Conference on Biological Effects of Microwave Energy, University of Virginia, p. 146, (1958)

40. Carpenter, R. L., "An Experimental Study of the Biological Effects of Microwave Radiation in Relation to the Eye," RADC-TDR-62-131: (1962)

41. Richardson, A. W., Duane, T. D., and Hines, H. M., "Experimental Cataract Produced by 3 cm Pulsed Microwave Radiation," Arch Ophth., 45: 382, (1951)

42. Carpenter, R. L. and Van Ummersen, C. A., "The Action of Microwave Radiation on the Eye," The Journal of Microwave Power 3: 3, (1969)

43. Lidman, B., and Cohn, C., "Effects of Radar Emanations on the Hematopoietic System," Air Surgeon's Bulletin, 2: 448, (1945)

44. Livshits, N. N., "The Role of the Nervous System in Reactions to UHF Electromagnetic Fields," Biofizika 2: 372, (1957)

45. Livshits, N. N., "The Effect of an Ultra-High Frequency Field on the Functions of the Nervous System," Biofizika 3: 409, (1958)

46. Presman, A. S. and Levitina, N. A., "Non-thermal Action of Microwaves on Cardiac Rhythm," Byulleten Eksperimental noi Biologü i Meditsiny 53: 41, (1962)

47. Letavet, A. A. and Gordon, Z. J., "The Biological Action of Ultra-High Frequencies," Academy of Medical Sciences, USSR, Moscow, (1960)

48. Kamenskiy, Yu.I., "Influence of Microwaves on the Functional Condition of the Nerve," Biofizika 9: 695, 1964 Translation ATD Report T-65-39

49. Dodge, C. and Kassel, S., "Soviet Research on the Neural Effects of Microwaves," ATD Report 66-133, Library of Congress, (1966)

50. Soviet Biotechnology and Bioastronautics, ATD Report 67-17, Library of Congress, (1967)

51. Eakin, S. K. and Thompson, W. D., "Behavioral Effects of Stimulation by UHF Radio Fields," Psychological Reports 17: 595, (1965)

52. Tanner, J. A., Romero-Sierra, C. and Davie, S. J., "Non-thermal Effects of Microwave Radiation on Birds," Nature 216: 1139, (1967)

53. Deichmann, W. B., "Biological Effects of Microwave Radiation of 24,000 Megacycles," Archiv für Toxikologie 22: 24, (1966)

54. Michaelson, S. M., Thomson, R. A. E., El Tamami, M. Y., Seth, H. S. and Howland, J. W., "The Hematologic Effects of Microwave Exposure," Aerospace Medicine: 824, Sept., (1964)

55. Gorodetskaia, S. F., "The Influence of an SHF Electromagnetic Field on the Reproduction, Composition of Peripheral Blood, Conditioned Reflex Activity, and Morphology of the Internal Organs of White Mice," In A. A. Gorodetskiy, Biological Action of Ultrasound and Super-high Frequency Electromagnetic Oscillations, Academy of Sciences, Kien, (1964)

56. Sigler, A. T., Lebienfeld, A. M., Cohen, B. H., and Westlake, J. E., Bulletin Johns Hopkins Hospital 117: 374, (1965)

57. Loshak, A. Ya., "The Problem of the Combined Biological Effects of X-Ray and UHF Irradiation," Problemy Kosmicheskoy Meditsiny (Problems of Space Medicine), 262, Moscow (ATD Report 66-116)

58. Michaelson, S. M., Thomson, R. A. E., Odland, L. T. and Howland, J. W., "The Influence of Microwaves on Ionizing Radiation Exposure," Aerospace Medicine 34: 111, (1963)

59. Thomson, R. A. E., Michaelson, S. M. and Howland, J. W., "Leukocyte Response Following Simultaneous Ionizing and Microwave (Radar) Irradiation," Blood 28: 157, (1966)

60. Presman, A. S. and Levitina, N. A., "The Effect of Non-thermal Microwave Radiation on the Resistance of Animals to Gamma-Irradiation," Radiobiologiya 2: 170, (1962), FTD-TT-62-667

61. Howland, J. W., Michaelson, S. M., Thomson, R. A. E. and Mermagen, H., "The Effect of Microwaves on the Response to Ionizing Radiation," RADC-TDR-62-102, (1962)

62. Thomson, R. A. E., Michaelson, S. M. and Howland, J. W., "Microwave Radiation and Its Effect on Response to X-Radiation," Aerospace Medicine: 252, March 1967

63. Michaelson, S. M., Thomson, R. A. E. and Quinlan, W. J., Jr., "Effects of Electromagnetic Radiations on Physiologic Responses," Aerospace Medicine: 293, March 1967

64. Lamb, J. C., Isaacs, J. P., Bloom, W. L. and Harmer, D. S., "Electrical Thrombosis of Blood Vessesl: A Voltage-Dependent Phenomenon," Am. J. Physiol. 208: 1006, (1965)

65. Richardson, A. W., "Blood Coagulation Changes due to Electromagnetic Microwave Irradiation," Blood 14: 1237, (1959)

66. Teeter, W. L. and Bushore, K. R., "A Variable-Ratio Microwave Power Divider and Multiplexer," IRE Transactions on Microwave Theory and Techniques: 227, October 1957

67. Silver, S., Microwave Antenna Theory and Design, Boston Technical Lithographers, Inc., Lexington, Mass., 189 (1963)

68. Bassett, H. L. and Bomar, S. H., Jr., "Dielectric Constant and Loss Tangent Measurement of High Temperature Electromagnetic Window Materials," Technical Report No. AFWL-TR-69-92, Georgia Institute of Technology, Atlanta, Ga., Dec. 1969

69. Primich, R. I. and Hayami, R. A., "Millimeter Wavelength Focused Probes and Focused, Resonant Probes for Use in Studying Ionized Waves Behind Hypersonic Velocity Projectiles," ARPA Order No. 347-463, AD 413 158, July 1963

70. Marshall, S. L., Laser Technology and Applications, McGraw-Hill Book Company, Inc., New York, N. Y., 238, (1968)

71. Senior, T. B. A., Plonus, M. A. and Knott, E. F., "Designing Foamed-Plastic Target Supports," Microwaves: 38, December 1964

72. Jasik, H., Antenna Engineering Handbook, McGraw-Hill Book Company, Inc., New York, N. Y., (1961)

73. Hougie, C., Fundamentals of Blood Coagulation in Clinical Medicine, McGraw-Hill Book Company, Inc., New York, N. Y. (1963)

74. Zucker, M. B., "Blood Platelets," Scientific American, 204: 58, (1961)

75. Bowie, E. J. W., Thompson, J. H. and Owen, C. A., Jr., Proc. Mayo Clinic 40: 625, (1965)

76. Born, G. V. R., Plenary Session Papers, XII Congress, International Soc. Hematol., New York, (1968) p. 95

77. Hemker, H. C., Loelinger, E. A. and Veltkamp, J. J., Human Blood Coagulation, Springer-Verbag New York, Inc., New York, N. Y., 162, (1969)

78. Altschuler, H. M., "Dielectric Constant" in Handbook of Microwave Measurements, ed. by Sucher and Fox, Polytechnic Press of the Polytechnic Institute of Brooklyn, New York, N. Y., 2:503, (1963)

79. von Hippel, A. R. Dielectric Materials and Applications, The M.I.T. Press, Cambridge, Mass., 86, (1966)

80. Richmond, J. H.,"Calculation of Transmission and Surface Wave Data for Plane Multilayers and Inhomogeneous Plane Layers," AD 427 030 31 October 1963

81. Breeden, K. H.,"Millimeter Radome Design Techniques," AFAL-TR-68-38, Georgia Institute of Technology, Atlanta, Ga., February 1968

VITA

Richard F. Boggs was born in Elmira, New York, in 1937 and graduated from the Elmira Free Academy in 1955. He received a B.C.E. Degree in 1959 from Rensselaer Polytechnic Institute and a M.S. Degree in Nuclear Engineering in 1966 from the Georgia Institute of Technology.

When receiving his Bachelor's Degree, he was commissioned a 2nd Lieutenant in the U.S. Air Force, and served for three years as the Sanitary and Industrial Hygiene Engineer at Olmsted Air Force Base, Pennsylvania.

In 1962, Mr. Boggs entered on duty with the commissioned corps of the U.S. Public Health Service and was assigned to the Radiological Health Laboratory of the then Division of Radiological Health at Rockville, Maryland. He was with the Radiation Surveillance Program until 1963 when he was assigned to the Radioactive Materials Section. In 1964, he received approval to pursue his graduate studies and, in 1964 and 1965, attended the School of Nuclear Engineering at Georgia Tech. He returned to the USPHS Rockville Laboratory in 1965 and established the Particle Accelerator Program. This was expanded and Mr. Boggs was appointed Chief of the Industrial Radiation Section. In 1967, he was appointed Chief, Radioactive Materials Branch. He remained in this position until June, 1969, when he again received approval for support of graduate work and returned to the Georgia Tech School of Nuclear Engineering.

His publications include:

"Development of an Incident Data Collection and Processing System," USPHS, Division of Radiological Health Publication, September, 1963.

"Summary of the Public Health Service Film Badge Program," USPHS, Bureau of Radiological Health Publication, February, 1964.

Health Physics Aspects of the Operation of Cockroft-Walton Type Neutron Generators, USPHS, DRH Publication, March, 1966.

"PHS Activities Concerning Tritium Hazards Associated with Neutron Generators," Abridged Proceedings of the Symposium on Instrumentation, Experience, and Problems in Health Physics Tritium Control, Sandia Corporation, Albuquerque, New Mexico, June, 1967, p. 45.

A Summary Report on X-Ray Diffraction Equipment, PHS, National Center for Radiological Health, MORP Report 67-5, June, 1967.

"Health and Safety Aspects of Industrial Radiography," Journal of the American Society of Safety Engineers, Vol. 12, No. 11, November, 1967, coauthor.

Tritium Contamination in Particle Acclerator Operation, PHS Environmental Health Series, No. 999-RH-29, November, 1967, coauthor.

Recommendations for the Safe Operation of Particle Accelerators, USPHS, NCRH MORP Report 68-2, February, 1968, coauthor.

"Industrial Exposure to Radiation," Guidelines to Radiological Health, PHS Environmental Health Series, No. 999-RH-33, September, 1968, p. 157, coauthor.

"Radiological Health Aspects of the Control of Spent Radon Seeds," Radiological Health Data and Reports, Vol. 10, No. 5, May, 1969, coauthor.

Mr. Boggs received his Professional Engineering license in New York State in 1966, was certified in 1968 by the Environmental Engineering Intersociety Board, and is a Diplomate in the American Academy of Environmental Engineers.

Mr. Boggs was appointed the PHS liaison officer to the American National Standards Institute and served on the N43 Committee, Equipment for Non-Medical Radiation Applications, and Subcommittee N43.4 on Particle Accelerators. He served as Secretary-Treasurer of the Conference

on Radiological Health from 1965 to 1967 and on the Executive Committee from 1967 to 1969. In 1969 and 1970, he was elected Secretary of the Georgia Tech Student Branch of the American Nuclear Society.

Mr. Boggs is a member of the Health Physics Society, the American Public Health Association, the American Industrial Hygiene Association, American Conference of Governmental Industrial Hygienists, the American Nuclear Society, and the Society of the Sigma Xi. He is married to the former Ardith Gunderman and has a son, Glenn, and daughter, Dana.